Astron. Astrophys. 332, 877–903 (1998)

ASTRONOMY AND ASTROPHYSICS

Insights into the formation of barium and Tc-poor S stars from an extended sample of orbital elements⋆,⋆⋆

A. Jorissen[1,2⋆⋆⋆], **S. Van Eck**[1,3], **M. Mayor**[3], **and S. Udry**[3]

[1] Institut d'Astronomie et d'Astrophysique, Université Libre de Bruxelles, C.P.226, Boulevard du Triomphe, B-1050 Bruxelles, Belgium
[2] Department of Astrophysical Sciences, Princeton University, Princeton, New Jersey, USA
[3] Observatoire de Genève, CH-1290 Sauverny, Switzerland

Received 27 August 1997 / Accepted 19 September 1997

Abstract. The set of orbital elements available for chemically-peculiar red giant (PRG) stars has been considerably enlarged thanks to a decade-long CORAVEL radial-velocity monitoring of about 70 barium stars and 50 S stars. When account is made for the detection biases, the observed binary frequency among strong barium stars, mild barium stars and Tc-poor S stars (respectively 35/37, 34/40 and 24/28) is compatible with the hypothesis that they are all members of binary systems. The similarity between the orbital-period, eccentricity and mass-function distributions of Tc-poor S stars and barium stars confirms that Tc-poor S stars are the cooler analogs of barium stars.

A comparative analysis of the orbital elements of the various families of PRG stars, and of a sample of chemically-normal, binary giants in open clusters, reveals several interesting features. The eccentricity – period diagram of PRG stars clearly bears the signature of dissipative processes associated with mass transfer, since the maximum eccentricity observed at a given orbital period is much smaller than in the comparison sample of normal giants. The mass function distribution is compatible with the unseen companion being a white dwarf (WD). This lends support to the scenario of formation of the PRG star by accretion of heavy-element-rich matter transferred from the former asymptotic giant branch progenitor of the current WD. Assuming that the WD companion has a mass in the range 0.60 ± 0.04 M$_\odot$, the masses of mild and strong barium stars amount to 1.9 ± 0.2 and 1.5 ± 0.2 M$_\odot$, respectively. Mild barium stars are not restricted to long-period systems, contrarily to what is expected if the smaller accretion efficiency in wider systems were the dominant factor controlling the pollution level of the PRG star. These results suggest that the difference between mild and strong barium stars is mainly one of galactic population rather than of orbital separation, in agreement with their respective kinematical properties.

There are indications that metallicity may be the parameter blurring the period – Ba-anomaly correlation: at a given orbital period, increasing levels of heavy-element overabundances are found in mild barium stars, strong barium stars, and Pop.II CH stars, corresponding to a sequence of increasingly older, i.e., more metal-deficient, populations. PRG stars thus seem to be produced more efficiently in low-metallicity populations. Conversely, normal giants in barium-like binary systems may exist in more metal-rich populations. HD 160538 (DR Dra) may be such an example, and its very existence indicates at least that binarity is not a sufficient condition to produce a PRG star.

Key words: stars: late-type – stars: chemically peculiar – stars: abundances – binaries: spectroscopic

1. Introduction

Barium stars were identified as a class of peculiar red giants by Bidelman & Keenan (1951). Typical chemical peculiarities exhibited by these G and K giants include overabundances of carbon and of elements heavier than Fe, like Ba and Sr (e.g. Lambert 1985). These elements bear the signature of the s-process of nucleosynthesis, a neutron-capture chain starting on Fe seed nuclei and synthesizing nuclides heavier than Fe located along the valley of nuclear stability (Burbidge et al. 1957). The operation of the s-process is commonly associated with He-burning thermal pulses occurring on the asymptotic giant branch (AGB). As a result of the so-called 'third dredge-up', s-process enriched material is brought to the surface of the AGB star (Iben & Renzini 1983; Sackmann & Boothroyd 1991). Barium stars, as well as their Pop.II counterparts, the CH stars (first introduced by Keenan in 1942), are too warm and of too low a luminosity to have undergone third dredge-ups on the AGB (e.g. Scalo 1976; Bergeat & Knapik 1997). With the discovery of the binary nature of these stars (McClure et al. 1980; McClure 1983), their chemical peculiarities have been attributed to mass transfer across the binary system. When the current WD companion of the barium star was a thermally-pulsing AGB star, it transferred s-process- and C-rich material onto its companion, which is now viewed as a barium or CH star.

Send offprint requests to: A. Jorissen (at the address in Belgium)

⋆ This paper is dedicated to the memory of Antoine Duquennoy, who contributed many among the observations used in this study

⋆⋆ Based on observations carried out at the European Southern Observatory (ESO, La Silla, Chile), and at the Swiss telescope at Haute Provence Observatory

⋆⋆⋆ Research Associate, National Fund for Scientific Research (FNRS), Belgium

The exact way by which the matter was transferred from the AGB star onto its companion – either by wind accretion in a detached binary, or by Roche lobe overflow (RLOF) in a semi-detached binary – is still a matter of debate. On one hand, the fact that barium stars have non-circular orbits points against RLOF in a semi-detached system, as tidal effects will efficiently circularize the orbit when the giant is about to fill its Roche lobe. But on the other hand, RLOF seems unavoidable for the barium stars with the shortest periods, since their orbital separation is too small to have accomodated a large AGB star in a detached binary system in the past (see in particular the case of HD 121447, having the second shortest orbital period among barium stars; Jorissen et al. 1995). The main difficulty with RLOF is that, when this process involves a giant star with a convective envelope, it is expected to lead to a dramatic orbital shrinkage. This so-called 'case C' mass transfer is dynamically unstable when the mass-loser is the more massive star in the system. A common envelope generally forms at that stage, causing a strong drag on the embedded stars (e.g. Meyer & Meyer-Hofmeister 1979; Iben & Tutukov 1993). A way out of this dilemna has recently been proposed by Han et al. (1995), by pointing out that, under some special conditions, the dynamical instability associated with case C mass transfer can be avoided.

The present paper contains an extensive analysis of the orbital elements of barium stars, since the new orbits presented in companion papers (Udry et al. 1998ab) considerably enlarge the database, from the 17 orbits from McClure & Woodsworth (1990) that were available to Han et al. (1995) to more than 50 now. The binary evolution channels relevant for barium stars, as identified by Han et al. (1995), will be confronted with our new data, with special emphasis on the $(e, \log P)$ diagram. The number of available orbits is now large enough to perform a meaningful comparison of the period and mass-function distributions of strong and mild barium stars.

As far as S stars are concerned, it has become clear that Tc-rich and Tc-poor S stars form two separate families with similar chemical peculiarities albeit of very different origins (Iben & Renzini 1983; Little et al. 1987; Jorissen & Mayor 1988; Smith & Lambert 1988; Brown et al. 1990; Johnson 1992; Jorissen & Mayor 1992; Groenewegen 1993; Johnson et al. 1993; Jorissen et al. 1993; Ake 1997). Tc-rich (or 'intrinsic') S stars are genuine thermally-pulsing AGB stars where the s-process operates in relation with the thermal pulses, and where the third dredge-up brings the freshly synthesized s-elements (including Tc) to the surface (e.g. Iben & Renzini 1983; Sackmann & Boothroyd 1991). By contrast, Tc-poor (or 'extrinsic') S stars are believed to be the cool descendants of barium stars. The evolutionary link between barium and S stars is discussed in the light of the 25 orbits now available for S stars, and appears to be fully confirmed.

Finally, we present some suggestions to solve the dilemna expressed above about the mass transfer mode that operated in barium and extrinsic S stars.

2. The stellar samples

Radial-velocity monitoring of several samples of chemically-peculiar red giants (PRG) has been performed by the team of McClure at the Dominion Astrophysical Observatory (DAO, Canada) and by the CORAVEL team on the Swiss 1-m telescope at Haute-Provence Observatory (France) and on the Danish 1.54-m telescope at the European Southern Observatory (La Silla, Chile), with the aim of deriving their binary frequencies. A detailed description of the CORAVEL data, along with the new orbits, is given in two companion papers (Udry et al. 1998ab; see Baranne et al. 1979 for a description of the CORAVEL spectro-velocimeter).

A brief description of these samples, on which the present study relies, is given below, with special emphasis on their statistical significance.

2.1. Barium stars with strong anomalies

The CORAVEL and DAO samples taken together contain *all 34 known barium stars with strong anomalies* (i.e. Ba4 or Ba5 on the scale defined by Warner 1965) from the list of Lü et al. (1983). The binary frequency derived for this complete sample in Sect. 4 thus allows us to address the question of whether binarity is a necessary condition to form a strong barium star. Three stars with a Ba3 index monitored by McClure were included as well in this sample of strong barium stars.

2.2. Barium stars with mild anomalies

The CORAVEL and DAO samples taken together include 40 stars with a mild barium anomaly (Ba$<$1, Ba1 and Ba2 on the scale of Warner 1965). The CORAVEL sample is a random selection of 33 Ba$<$1, Ba1 and a few Ba2 stars from the list of Lü et al. (1983). Although this sample is by no means complete, it provides a good comparison to the sample of strong barium stars described above, for investigating the correlation between the orbital elements and the intensity of the chemical anomaly.

Because orbital elements for barium stars are spread in the literature, Tables 1a and 2a collect all orbital elements available for mild and strong barium stars, respectively. The number in column 'Ref.' of these tables refers to the following papers where the complete set of orbital elements for the considered star can be found: 0. This paper (see below); 1. Udry et al. (1998a); 2: Udry et al. (1998b); 5. Griffin (1996); 6. Griffin et al. (1996); 7. Jorissen et al. (1995); 11. Griffin & Keenan (1992); 12. Griffin (1991); 13. McClure & Woodsworth (1990); 20: Griffin & Griffin (1980). Fekel et al. (1993) report preliminary orbital elements for the mild barium star HD 165141; the lower limit on the orbital period quoted in Table 1a is derived from their more accurate KPNO data. For the sake of completeness, a note identifies stars with an orbital or acceleration solution in the Hipparcos Double and Multiple Systems Annex (ESA 1997). The comparison between the astrometric and spectroscopic elements is deferred to a future study.

Table 1a. Orbital elements for mild (Ba<1, Ba1 and Ba2) barium stars. Column 2 provides the spectral subclass (> 0 if K type, < 0 if G type) and column 3 the Ba index, from Lü et al. (1983). The columns labeled $\bar{\epsilon}_1$ and N give the average error on one measurement and the number of measurements, respectively. A dash in column Sb indicates that the spectral line width is smaller than the instrumental profile. For orbits obtained from instruments other than CORAVEL, the Sb parameter is not available ('na'). When an orbital solution is available, γ is the systemic radial velocity; otherwise, it is the average radial-velocity with its standard deviation. $\Delta(38-41)$ is a photometric index characterizing the strength of the Ba anomaly (see text). The numbers in column 'Ref.' refer to Table 5, which gives the reference where the complete set of orbital parameters for the considered system may be found

HD/DM	Sp.	Ba	P (d)	e	$f(M)$ ($M_\odot$)	$O-C$ (km/s)	$\bar{\epsilon}_1$ (km/s)	N	S_b (km/s)	γ (km/s)	$\Delta(38-41)$	Ref.
22589	-5	<1	5721.2±454	0.24±0.17[a]	0.0042±0.0025	0.22	0.37	19	1.1	−28.0±0.6	−0.03	1
26886	-8	1	1263.2±3.7	0.39±0.02	0.025 ±0.002	0.40	0.32	23	2.0	+3.8±0.1	+0.02	2
27271	-8	1	1693.8±9.1	0.22±0.02	0.024 ±0.001	0.31	0.30	23	1.2	−18.1±0.1	−0.01	2
40430	0	1	>3700				0.34	15	1.7	−23.9±1.0	−0.03	1
49841	-8	1	897.1 ±1.8	0.16±0.01	0.032 ±0.002	0.33	0.32	21	1.0	+10.9±0.1	−0.09	2
51959[g]	2	1	>3700				0.34	21	–	+38.9±0.8	+0.07	1
53199	-8	2	7500	0.21±0.22[a]	0.026 ±0.001	0.17	0.36	11	1.1	+23.3±0.1	−0.07	2
58121	0	1	1214.3±5.7	0.14±0.02	0.015 ±0.001	0.24	0.30	23	1.3	+10.2±0.1	−0.04	2
58368	0	2	672.7 ±1.3	0.22±0.02	0.021 ±0.001	0.39	na	31	na	+37.8±0.1	−0.11	13
59852	-9	1	3463.9±53.8	0.15±0.06	0.0022±0.0004	0.27	0.34	19	–	+0.1±0.1	−0.10	1
77247[c,d]	-5	1	80.53 ±0.01	0.09±0.01	0.0050±0.0001	0.50	na	66	5.8	−19.7±0.1	na	0,13
91208	0	1	1754.0±13.3	0.17±0.02	0.022 ±0.002	0.39	0.32	24	0.7	+0.2±0.1	−0.05	1
95193	0	1	1653.7±9.0	0.13±0.02	0.026 ±0.001	0.26	0.32	18	0.8	−7.3±0.1	−0.06	1
98839[b]	-7	<1	>11000					56	na	−1:	na	5
101079	1	1	>1500				0.34	7	1.2	−2.2±0.2	−0.17	2
104979	0	1	>4700				0.29	25	0.7	−30.8±0.4	+0.07	2
131670[c,e]	1	1	2929.7±12.2	0.16±0.01	0.040 ±0.002	0.36	0.30	55	0.6	−25.1±0.1	−0.13	1,13
134698	1	1	>3600				0.33	22	0.5	−29.5±1.6	−0.20	1
139195	1	1	5324 ±19	0.35±0.02	0.026 ±0.002	0.7	na	107	–	+6.3±0.1	−0.02	12
143899	-8	1	1461.6±6.9	0.19±0.02	0.017 ±0.001	0.27	0.35	26	0.3	−29.8±0.1	−0.05	1
165141	0	1	>2100					10	na	+10.2±1.8	−0.14	4,23
180622	1	1	4049.2±37.7	0.06±0.10[a]	0.070 ±0.020	0.25	0.30	10	–	+39.2±1.1	−0.10	2
196673[c,d]	2	2	6500	0.64±0.03	0.013 ±0.002	0.47	0.5	51	3.0	−24.6±0.1	0.00	1,13
199394[c,d]	-8	1	4606.5±351[f]	0.06±0.06[a]	0.023 ±0.003	0.40	na	52	1.1	−5.6±0.2	−0.15	0,13
200063	3	1	1735.4±8.1	0.07±0.04[a]	0.058 ±0.004	0.23	0.29	10	2.3	−58.3±0.2	−0.10	2
202109[g]	-8	1	6489.0±31.0	0.22±0.03	0.023 ±0.003	0.8	na	112	0.0	+16.7±0.1	−0.06	11
204075[c,d]	-5	2	2378.2±55	0.28±0.07	0.004 ±0.001	0.52	na	32	4.9	+2.1±0.1	−0.15	0,13
205011[c,d]	1	1	2836.8±10	0.24±0.02	0.034 ±0.003	0.45	na	41	1.4	+11.5±0.1	−0.13	0,13
210946	1	1	1529.5±4.1	0.13±0.01	0.041 ±0.001	0.26	0.31	30	1.3	−4.3±0.1	−0.11	2
216219	-1	1	4098.0±111.5	0.10±0.04	0.013 ±0.001	0.37	0.33	29	2.0	−7.2±0.1	−0.07	2
223617[c,d,g]	2	2	1293.7±3.9	0.06±0.02	0.0064±0.0004	0.34	na	39	0.4	+28.5±0.1	−0.10	2,13
288174	0	1	1824.3±7.1	0.19±0.01	0.017 ±0.001	0.15	0.33	14	0.9	+34.7±0.1	−0.12	1
$-01°3022$	1	1	3252.5±31.4	0.28±0.02	0.016 ±0.001	0.25	0.36	26	1.0	−35.4±0.1	−0.15	1
$-10°4311$	-0	1	>3400				0.45	33	1.5	+52.7±2.9	−0.14	1
$-14°2678$	0	<1	3470.5±107	0.22±0.04	0.023 ±0.002	0.39	0.38	15	2.9	+4.9±0.1	+0.06	1

Remarks:
a: data compatible with circular orbit at 5% confidence level (Lucy-Sweeney test);
b: not listed in Lü et al. (1983), but present in Lü (1991);
c: Combined CORAVEL/DAO orbit;
d: A DAO-CORAVEL offset of -0.46 km s^{-1} has been applied to the DAO measurements;
e: A DAO-CORAVEL offset of -0.73 km s^{-1} has been applied to the DAO measurements;
f: A somewhat more accurate period (4382 ± 91 d) is obtained by forcing $e = 0$;
g: Acceleration solution listed in the Hipparcos Double and Multiple Systems Annex (ESA 1997)

For several barium stars monitored by McClure, a few CORAVEL measurements have been obtained to improve the DAO orbit, since these measurements significantly increase the time span of the monitoring. These updated orbits are listed in Table 1a and 2a under the reference number 0. A zero-point correction of -0.46 km s^{-1} has been applied to the DAO measurements, as derived from the average difference in systemic

Table 1b. Suspected binary mild barium stars. The numbers in column 'Ref.' refer to the papers listed in Table 5

HD	Sp.	Ba	N	Δt (d)	V_r (km/s)	$\sigma(V_r)$ (km/s)	$\bar{\epsilon}_1$ (km/s)	S_b (km/s)	$\Delta(38-41)$	Ref.	Rem.
18182	0	0	22	3451	25.76	0.45	0.32	–	−0.03	0	
183915	0	2	9	4073	−50.08	0.50	0.29	0.3	−0.18	0,13	
218356	2	2	13	6201	−27.86	1.17	0.29	3.6	−0.13	0,19	56 Peg (K0IIp + WD)

Table 1c. Mild barium stars with no evidence of binary motion. The numbers in column 'Ref.' refer to the papers listed in Table 5

HD	Sp.	Ba	N	Δt (d)	V_r (km/s)	$\sigma(V_r)$ (km/s)	$\bar{\epsilon}_1$ (km/s)	S_b (km/s)	$\Delta(38-41)$	Ref.	Rem.
50843	1	1	20	4437	12.21	0.33	0.33	–	−0.03	0	
95345	2	1	26	3036	5.48	0.21	0.28	0.7	+0.07	0	
119185	0	1	17	2869	−74.51	0.24	0.36	0.8	−0.05	0	
130255	0	1	26	2956	40.19	0.33	0.32	–	+0.01	0,9	subgiant CH

Table 1d. Supergiants misclassified as mild barium stars. The numbers in column 'Ref.' refer to the papers listed in Table 5

HD	Sp.	Ba	N	Δt (d)	V_r (km/s)	$\sigma(V_r)$ (km/s)	$\bar{\epsilon}_1$ (km/s)	S_b (km/s)	$\Delta(38-41)$	Ref.	Rem.
65699	0	0	21	5163	11.17	0.27	0.31	6.0	−0.01	0,16	
206778	2	1	94	6204	2.82	0.56	0.27	5.8	+0.06	0,16	ϵ Peg (K2II/Ib var)

velocity for the 3 stars (HD 46407, HD 131670 and HD 223617) for which independent DAO and CORAVEL orbits are available.

Several barium stars have very long periods, exceeding the time span of the monitoring. In those cases, whenever possible, a preliminary orbit was nevertheless derived by fixing one of the orbital parameters (usually the period). Those cases can be readily identified in Tables 1a and 2a by the fact that there is no uncertainty given for the fixed parameter (see Udry et al. 1998a for more details).

2.3. Non-variable S stars

Besides the orbit obtained for the S star HR 1105 (=HD 22649) by Griffin (1984), our CORAVEL monitoring of a sample of 56 S stars is the primary source for investigating the binary frequency among S stars. This sample includes 36 bright, northern S stars from the *General Catalogue of Galactic S Stars* (GCGSS; Stephenson 1984) *with no variable star designation*, neither in the *General Catalogue of Variable Stars* (Kholopov et al. 1985) nor in the *New Catalogue of Suspected Variable Stars* (Kukarkin et al. 1982). The criterion of photometric stability has been adopted to avoid the confusion introduced by the envelope pulsations masking the radial-velocity variations due to orbital motion. Such a selection criterion clearly introduces a strong bias against intrinsically bright S stars, which is of importance when deriving the binary frequency among S stars (see the discussion in Sect. 4.3).

Our samples include the border case HD 121447, sometimes classified as a Ba5 star and sometimes as an S star; in the analysis of the orbits presented in the next sections, this star has been included among *both* barium and S stars.

Table 3a presents all 25 orbits available for S stars, collected from the following papers, referred to in column 'Ref.' of Table 3a: 0. This paper (see below); 1. Udry et al. (1998a); 3. Carquillat et al. (1998); 7: Jorissen et al. (1995); 10: Jorissen & Mayor (1992); 18: Griffin (1984). The orbits of Jorissen & Mayor (1992) have been updated with a few new measurements and listed in Table 3a with reference number 0 in column 'Ref'.

2.4. Mira S stars

A sample of 13 Mira S stars has also been monitored with CORAVEL, in order not to restrict the search for binaries to low-luminosity S stars (see Sect. 2.3). However, the envelope pulsations of Mira stars will undoubtedly hamper that search (see Sect. 3 and Udry et al. 1998a for a detailed discussion).

2.5. SC and Tc-poor carbon stars

A sample of 7 SC and CS stars has been monitored as well with CORAVEL, along with the 3 carbon stars lacking Tc from the list of Little et al. (1987).

2.6. CH stars

Orbits of CH stars are provided by McClure & Woodsworth (1990), and are not repeated here.

Table 2a. Same as Table 1a for strong (Ba3, Ba4 and Ba5) barium stars. The numbers in column 'Ref.' refer to the papers listed in Table 5

HD/DM/ others	Sp.	Ba	P (d)	e	$f(M)$ ($M_\odot$)	$O-C$ (km/s)	$\bar{\epsilon}_1$ (km/s)	N	S_b (km/s)	γ (km/s)	Δ $(38-41)$	Ref.
5424	1	4	1881.5±18.6	0.23 ±0.04	0.005 ±0.0004	0.18	0.30	13	–	−0.3±0.1	−0.11	1
16458[g]	1	5	2018 ±12	0.10 ±0.02	0.041 ±0.003	0.38	na	36	na	+20.3±0.1	−0.13	13
20394	0	4	2226 ±22	0.20 ±0.03	0.0020±0.0002	0.34	-	87	–	+24.2±0.1	−0.09	6
24035	4	4	377.8 ±0.3	0.02 ±0.01[a]	0.047 ±0.003	0.19	0.29	15	–	−12.5±0.1	−0.26	1
31487	1	5	1066.4±2.6	0.05 ±0.01	0.038 ±0.002	0.33	na	35	na	−4.2±0.7	na	13
36598	2	4	2652.8±22.7	0.08 ±0.02	0.037 ±0.002	0.21	0.27	11	–	+44.1±0.1	−0.18	1
42537	4	5	3216.2±54.7	0.16 ±0.05	0.027 ±0.005	0.43	0.30	12	1.9	−2.5±0.2	−0.31	1
43389	2	5	1689.0±8.7	0.08 ±0.02	0.043 ±0.002	0.35	0.32	24	0.6	+53.1±0.1	−0.16	2
44896	3	5	628.9 ±0.9	0.02 ±0.01[a]	0.048 ±0.001	0.21	0.26	19	1.9	+52.2±0.1	−0.17	2
46407[b,e]	0	3	457.4 ±0.1	0.013±0.008[a]	0.035 ±0.001	0.40	0.29	68	1.8	−3.4±0.1	−0.21	2,13
49641	1	3	1768 ±23	0.0	0.0031±0.0004	0.42	na	35	na	+4.4±0.1	−0.14	13
50082	0	4	2896.0±21.3	0.19 ±0.02	0.027 ±0.002	0.35	0.31	29	1.1	−17.4±0.1	−0.12	2
60197	3	5	3243.8±66.3	0.34 ±0.05	0.0028±0.0006	0.31	0.27	14	3.0	+54.3±0.1	−0.05	1
84678	2	4	1629.9±10.4	0.06 ±0.02[a]	0.062 ±0.003	0.30	0.29	12	0.8	+27.9±0.1	−0.31	1
88562	2	4	1445.0±8.5	0.20 ±0.02	0.048 ±0.003	0.44	0.32	23	0.7	+11.8±0.1	−0.04	1
92626	0	5	918.2 ±1.2	0.00 ±0.01[a]	0.042 ±0.002	0.32	0.27	35	0.5	+16.3±0.1	−0.29	2
100503	3	5	554.4 ±1.9	0.06 ±0.05[a]	0.011 ±0.001	0.55	0.28	16	1.7	−8.9±0.1	−0.22	1
101013[e]	0	5	1711 ±4	0.20 ±0.01	0.037 ±0.001	0.58	na	118	1.4	−14.5±0.1	−0.17	13,20
107541	0	4	3569.9±46.1	0.10 ±0.03	0.029 ±0.002	0.28	0.31	16	0.1	+88.1±0.1	−0.26	2
120620	0	4	217.2 ±0.1	0.01 ±0.01[a]	0.062 ±0.001	0.42	0.36	28	–	+33.2±0.1	−0.18	1
121447	7	5	185.7 ±0.1	0.015±0.013[a]	0.025 ±0.001	0.47	0.32	26	2.8	−11.9±0.1	−0.26	7
123949	6	4	9200	0.97 ±0.06	0.105 ±0.64	0.30	0.33	25	0.6	−10.8±0.3	−0.19	1
154430	2	4	1668.1±17.4	0.11 ±0.03[a]	0.034 ±0.003	0.48	0.29	15	1.3	−38.1±0.1	−0.04	1
178717	4	5	2866 ±21	0.43 ±0.03	0.006 ±0.001	0.47	na	46	2.0	−16.4±0.1	−0.20	13
196445	2	4	3221.3±43.0	0.24 ±0.02	0.031 ±0.002	0.23	0.29	12	0.6	−25.5±0.1	−0.22	1
199939	0	4	584.9 ±0.7	0.28 ±0.01	0.025 ±0.001	0.47	na	52	1.6	−41.7±0.1	−0.25	13
201657	1	4	1710.4±15.0	0.17 ±0.07	0.004 ±0.001	0.29	0.31	15	–	−27.7±0.2	−0.24	2
201824	0	4	2837 ±13	0.34 ±0.02	0.040 ±0.003	0.45	-	86	0.8	−31.1±0.1	−0.18	6
211594	0	4	1018.9±2.7	0.06 ±0.01	0.0140±0.0005	0.33	0.30	49	1.0	−9.9±0.1	−0.39	2
211954	2	5	5000	0.39 ±0.08	0.017 ±0.005	0.35	0.32	14	–	−6.1±0.1	−0.22	1
$+38^\circ 118$(a+b)[c]	2	5	299.4 ±0.2	0.14 ±0.01	0.0141±0.0004	0.30	0.31	30	1.4	−18.7±0.1	−0.19	1
$+38^\circ 118$(ab+c)[c]	2	5	3876.7±112.2	0.21 ±0.06	0.0017±0.0004	0.29	0.31	30	1.4	−18.3±0.1	−0.19	1
$-42^\circ 2048$	2	4	3260.0±28.3	0.08 ±0.02	0.065 ±0.004	0.24	0.29	12	1.4	+40.5±0.1	−0.16	1
$-64^\circ 4333$[d]	0	4	386.0 ±0.5	0.03 ±0.01[a]	0.068 ±0.003	0.31	0.33	16	–	+8.3±0.2	−0.29	1
Lü 163	−5	5	965.1 ±16.0	0.03 ±0.07[a]	0.0029±0.0006	0.57	0.39	14	–	+2.8±0.2	−0.39	1
NGC 2420 X	-	5	1402 ±10	0.0	0.050 ±0.005	0.50	na	16	–	+78.2±0.2	na	13,21

Remarks:
a: data compatible with circular orbit at 5% confidence level (Lucy-Sweeney test);
b: Combined CORAVEL/DAO orbit; A DAO-CORAVEL offset of -0.19 km s^{-1} has been applied to the DAO measurements;
c: triple system;
d: CpD;
e: Orbital solution listed in the Hipparcos Double and Multiple Systems Annex (ESA 1997);
g: Acceleration solution listed in the Hipparcos Double and Multiple Systems Annex (ESA 1997)

3. The radial-velocity jitter: a new diagnostic

The standard deviation of the $O-C$ residuals for some of the orbits computed by Udry et al. (1998ab) is clearly larger than expected from the error $\bar{\epsilon}_1$ on one measurement (Tables 1a, 2a and 3a). Fig. 1 shows that there is a tendency for the largest $O-C$ residuals to be found in the systems with the broadest spectral lines, as measured by the CORAVEL line broadening index Sb. The significance of this correlation is discussed in this section.

The CORAVEL spectrovelocimeter (Baranne et al. 1979) measures the stellar radial velocity by cross-correlating the stellar spectrum with a mask reproducing about 1500 lines of neutral and ionized iron-group species from the spectrum of Arcturus (K1III). Consequently, the width of the cross-correlation dip (cc-dip) is an indicator of line broadening. More precisely, the cc-dip of minor planets (reflecting the sun light), corrected for the solar rotational velocity and photospheric turbulence, allows the determination of an 'instrumental profile' σ_0. That parame-

Table 2b. Strong barium stars with no evidence for binary motion. The numbers in column 'Ref.' refer to the papers listed in Table 5

HD	Sp.	Ba	N	Δt (d)	V_r (km/s)	$\sigma(V_r)$ (km/s)	$\bar{\epsilon}_1$ (km/s)	S_b (km/s)	$\Delta(38-41)$	Ref.	Rem.
19014	4	5	18	3272	13.3	0.47	0.28	2.2	-0.01	0	jitter only?
65854	1	3	30	3369	0.5	0.42	na	na	na	13	

Table 3a. Orbital elements of S stars. Column 2, labeled GCGSS, lists the star number in the *General Catalogue of Galactic S Stars* (Stephenson 1984). The numbers in column 'Ref.' and 'Ref. Tc' refer to the papers listed in Table 5

HD/DM	GCGSS	Sp.	P (d)	e	$f(M)$ ($M_\odot$)	$O-C$ (km/s)	$\bar{\epsilon}_1$ (km/s)	N	S_b (km/s)	γ (km/s)	Ref. orb.	Tc	Ref. Tc	Rem.
7351	26	S3/2	4593 ±110	0.17 ±0.03	0.073 ±0.007	0.68	0.31	50	3.3	+1.5± 0.1	3,4	n	15	HR 363
22649[f]	79	S4/2	596.2 ±0.2	0.09 ±0.02	0.037 ±0.003	0.8	na	53	na	−22.3± 0.1	18	n	15	HR 1105
30959[d]	114	S3/1	> 1900				0.29	12	4.3	−8.8± 0.7	1,14	y	15	o^1 Ori
35155	133	S4,1	640.5 ±2.8	0.07 ±0.03	0.032 ±0.003	0.81[c]	0.33	19	3.5	+79.7± 0.2	0,10	n	15	
246818	156	S	2548.5±73.2	0.18 ±0.11[a]	0.0035±0.0015	0.59	0.37	17	2.8	−45.5± 0.2	1	n	8	$+05^\circ 1000$
288833	233	S3/2	> 3900				0.38	18	3.5	+81.1± 1.0	1	n	8	$+02^\circ 1307$
49368	260	S3/2	2995.9±67.1	0.36 ±0.05	0.022 ±0.003	0.58	0.34	23	4.3	+49.8± 0.1	1	n	15	V613 Mon
63733	411	S4/3	1160.7±8.9	0.23 ±0.03	0.025 ±0.003	0.38	0.32	14	3.5	+1.9± 0.1	1	y?	15	
95875	720	S3,3	197.2 ±0.4	0.02 ±0.04[a]	0.059 ±0.009	0.70	0.28	10	4.0	+40.6± 1.1	1	n	0	Hen 108
121447	-	S0	185.7 ±0.1	0.015±0.013[a]	0.025 ±0.001	0.47	0.32	26	2.8	−11.9± 0.1	7	n	17	
170970	1053	S3/1	4392 ±202	0.08 ±0.04[a]	0.021 ±0.002	0.33	0.30	39	3.9	−35.8± 0.1	1	y?	15	
184185	1140	S3*4	> 3400				0.43	22	4.3	+1.5± 1.6	1	-	-	$-21^\circ 5435$
191226	1192	M1S	1210.4±4.3	0.19 ±0.02	0.013 ±0.001	0.38	0.30	36	4.2	−25.0± 0.1	3	n	15	
191589	1194	S	377.3 ±0.1	0.25 ±0.003	0.394 ±0.005	0.29	0.30	41	3.1	−9.7± 0.1	1	n	15	
218634[e]	1322	M4S	> 3700				0.36	28	5.6	+20.1± 2.3	0,22	n	8	57 Peg
332077	1201	S3,1	669.1 ±1.0	0.077±0.007	1.25 ±0.02	0.66	0.46	39	10.2	−5.2± 0.1	0,10	n	8	
343486	1092	S6,3	3165.7±37.6	0.24 ±0.03	0.039 ±0.005	0.82	0.43	37	3.8	+4.9± 0.1	1	-	-	
$+21^\circ 255$[b]	45	S3/1	4137 ±317	0.21 ±0.04	0.032 ±0.004	0.51	0.33	36	3.2	−38.5± 0.3	1	n	8	
$+24^\circ 620$	87	S4,2	773.4 ±5.5	0.06 ±0.03[a]	0.042 ±0.005	0.82	0.41	19	4.0	−21.0± 0.2	0,10	n	8	
$+22^\circ 700$	96	S6,1	849.5 ±8.8	0.08 ±0.06[a]	0.043 ±0.008	1.14	0.48	20	4.9	+40.5± 0.3	0,10	n	8	
$+79^\circ 156$	106	S4,2	> 3900				0.39	19	4.3	−33.0± 2.1	1	n	8	
$+23^\circ 3093$	981	S5,4	1008.1±4.8	0.39 ±0.03	0.045 ±0.005	0.81	0.41	30	3.8	−44.1± 0.2	0,10	n	8	
$+23^\circ 3992$	1209	S3,3	3095.6±41.7	0.10 ±0.03[a]	0.034 ±0.004	0.71	0.37	43	4.3	−26.7± 0.1	1	n	8	
$+31^\circ 4391$	1267	S2/4	> 3600				0.37	28	3.3	+25.2± 1.6	1	-	-	
$+28^\circ 4592$	1334	S2/3:	1252.9±3.5	0.09 ±0.02	0.016 ±0.001	0.32	0.34	34	3.2	−37.5± 0.1	1	n	8	

Remarks:

a: Data compatible with circular orbit at 5% confidence level (Lucy-Sweeney test);

b: Visual binary; the S star is BD+21°255 = PPM 91178 = SAO 75009 = HIC 8876, whereas its visual K-type companion (BD+21°255p = PPM 91177 = SAO 75008) is also a spectroscopic binary whose orbit is given in Jorissen & Mayor (1992);

c: Two outlying measurements (at phase 0.38 and 0.93 deviating by 1.40 and -1.98 km s^{-1}, respectively) were kept in the present orbital solution. No obvious instrumental origin could be found to account for these outlying measurements, which may have a real - but as yet unidentified - physical cause in this strongly interacting system (Ake et al. 1991);

d: The WD companion of o^1 Ori has been detected by IUE (Ake & Johnson 1988);

e: 57 Peg has a composite spectrum S+A6V (Van Eck et al. 1998);

f: Orbital solution listed in the Hipparcos Double and Multiple Systems Annex (ESA 1997)

ter corresponds to the sigma of a gaussian function fitted to the cc-dip of a hypothetical star without rotation and turbulence. An estimator of the total broadening of stellar spectral lines can then be derived from the observed width σ of the stellar cc-dip as $Sb = (\sigma^2 - \sigma_0^2)^{1/2}$.

In cool red giants where macroturbulence is the main line-broadening factor, the Sb parameter is expected to increase with luminosity, as does macroturbulence (e.g. Gray 1988). This prediction is confirmed from the luminosities derived by Van Eck et al. (1998) from HIPPARCOS parallaxes for 23 S stars in common with the present sample. A least-square fit to these data yields the relation

$$M_{\rm bol} = -1.60 - 0.37\ Sb, \qquad (1)$$

valid for $3 \leq Sb \leq 9$ km s^{-1}. Since bright giants also exhibit large velocity jitters probably associated with envelope pulsations (e.g. Mayor et al. 1984), a correlation between Sb and the radial velocity jitter must indeed be expected, as observed

Table 3b. Non-binary (misclassified?) S stars

HD/DM	GCGSS	Sp.	N	Δt (d)	V_r (km/s)	$\sigma(V_r)$ (km/s)	$\bar{\epsilon}_1$ (km/s)	S_b (km/s)	Tc	Ref. Tc	Rem.
262427	247	S?	10	3622	+34.61	0.37	0.31	2.3	-	-	S class from Perraud (1959)
$+22^\circ4385$	1271	S2	26	3607	−2.63	0.36	0.36	2.6	-	-	S class from Vyssotsky & Balz (1958)

Table 3c. S stars with radial-velocity jitter. The numbers in column 'Ref. Tc' refer to the papers listed in Table 5

HD/DM	GCGSS	Sp.	N	Δt (d)	V_r (km/s)	$\sigma(V_r)$ (km/s)	$\bar{\epsilon}_1$ (km/s)	S_b (km/s)	Tc	Ref. Tc	Rem.
$BD-10^\circ1334$	176	Sr	16	3613	+22.72	1.39	0.48	7.1	-	-	
$BD+15^\circ1200$	219	S4/2	19	3933	+46.77	1.47	0.45	5.2	-	-	
61913	382	M3S	12	1860	−15.68	0.65	0.30	4.9	dbfl	17	NZ Gem = HR 2967
$BD-04^\circ2121$	416	S5/2	18	3585	+31.83	1.04	0.38	5.6	yes	8	
$BD-21^\circ2601$	554	S3*3	14	3308	+44.72	1.07	0.36	3.5	no	0	
$BD+20^\circ4267$	1158	Swk	19	3009	+26.69	1.59	0.41	6.9	-	-	
189581	1178	S4*2	19	3399	−17.04	0.78	0.34	4.5	no	15	
$BD+04^\circ4354$	1193	S4*3	13	3006	−8.79	0.63	0.39	5.3	yes	8	
192446	1198	S6/1	17	3245	−22.48	0.79	0.42	6.0	yes	8	
216672	1315	S4/1	30	3251	+12.47	0.76	0.31	4.9	yes	15	HR Peg = HR 8714

Table 3d. Mira S stars. The numbers in column 'Ref. Tc' refer to the papers listed in Table 5

HD	GCGSS	Var	Sp.	N	Δt (d)	V_r (km/s)	$\sigma(V_r)$ (km/s)	$\bar{\epsilon}_1$ (km/s)	S_b (km/s)	Tc	Ref. Tc	Rem.
1967	14	R And	S5-7/4-5e	9	1924	−4.85	4.92	0.54	9.6	yes	17	
4350	12	U Cas	S5/3e	5	729	−51.62	7.97	0.78	8.5	yes	17	
14028	49	W And	S7/1e	3	1856	−38.34	0.70	0.42	4.2	yes	17	
29147	103	T Cam	S6/5e	3	641	−11.09	5.28	0.55	11.5	yes	17	
53791	307	R Gem	S5/5	7	2126	−45.55	4.05	0.58	11.7	yes	17	
70276	494	V Cnc	S3/6e	4	2126	−4.71	10.17	0.48	10.3	dbfl	17	
110813	803	S UMa	S3/6e	13	2667	+1.46	5.15	0.45	10.1	yes	17	binary?
117287	-	R Hya	M6e-M9eS	16	2924	−9.69	2.06	0.70	9.6	prob	17	
185456	1150	R Cyg	S6/6e	4	767	−29.45	2.42	0.58	13.2	yes	17	
187796	1165	χ Cyg	S7/1.5e	12	2976	+3.24	3.19	0.61	8.3	yes	17	
190629	1188	AA Cyg	S6/3	31	2931	+11.41	1.33	0.42	8.7	yes	17	
195763	1226	Z Del	S4/2e	3	348	+37.43	3.52	0.93	9.7	yes	17	
211610	1292	X Aqr	S6,3e	7	1746	+11.67	7.20	0.75	8.3	prob	17	

Table 3e. SC Stars. The numbers in column 'Ref.' refer to the papers listed in Table 5

HD/DM	GCGSS	Var	Sp.	N	Δt (d)	V_r (km/s)	$\sigma(V_r)$ (km/s)	$\bar{\epsilon}_1$ (km/s)	S_b (km/s)	Tc	Ref. Tc	Rem.
286340	117	GP Ori	SC7/8	15	3614	+82.78	2.09	0.45	7.0	-	-	
44544	212	FU Mon	S7/7	17	3720	−25.86	1.71	0.48	7.2	-	-	
$BD-04^\circ1617$	244	V372 Mon	SC7/7	13	3341	+16.66	2.93	0.46	7.3	-	-	
$BD-08^\circ1900$	344		S4/6	17	3619	+72.47	1.54	0.40	5.4	-	-	binary?
54300		R CMi	CS	16	3740	+45.76	6.06	0.52	12.2	yes	17	pseudo-orbit
198164		CY Cyg	CS	27	3613	+4.52	1.02	0.34	6.9	yes	17	
209890		RZ Peg	C9	21	2932	−32.32	6.51	0.56	14.9	yes	17	pseudo-orbit

Table 4. Tc-poor carbon stars. The column labelled GCCCS refers to the entry number in the *General Catalogue of Cool Carbon Stars* (Stephenson 1973)

HD	GCCCS	Var	Sp.	N	Δt (d)	V_r (km/s)	$\sigma(V_r)$ (km/s)	$\bar{\epsilon}_1$ (km/s)	Sb (km/s)	Rem.
46687	537	UU Aur	C5,3	6	857	13.5	1.27	0.28	5.8	
76221	1338	X Cnc	C5,4	15	2117	−6.0	1.13	0.35	4.8	binary?
108105	1999	SS Vir	C6,3	16	1976	2.4	3.30	0.62	6.6	pseudo-orbit

Table 5. References to Tables 1-4

0	This paper
1	Udry et al. (1997a)
2	Udry et al. (1997b)
3	Carquillat et al. (1997)
4	Jorissen et al. (1996)
5	Griffin (1996)
6	Griffin et al. (1996)
7	Jorissen et al. (1995)
8	Jorissen et al. (1993)
9	Lambert et al. (1993)
10	Jorissen & Mayor (1992)
11	Griffin & Keenan (1992)
12	Griffin (1991)
13	McClure & Woodsworth (1990)
14	Ake & Johnson (1988)
15	Smith & Lambert (1988)
16	Smith & Lambert (1987)
17	Little et al. (1987)
18	Griffin (1984)
19	Schindler et al. (1982)
20	Griffin & Griffin (1980)
21	McClure et al. (1974)
22	Hackos & Peery (1968)
23	Fekel et al. (1993)

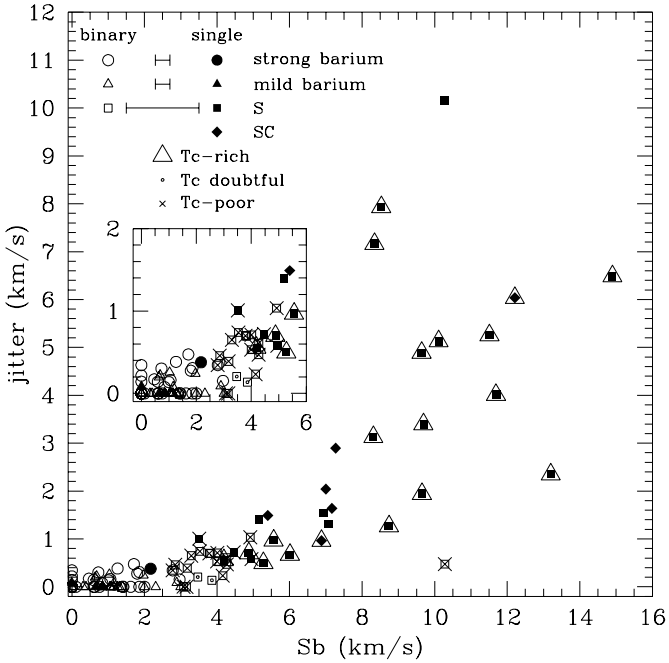

Fig. 1. The jitter $(\sigma^2 - \bar{\epsilon}_1^2)^{1/2}$ (where $\bar{\epsilon}_1$ is the average uncertainty on one measurement, and σ is the standard deviation of the radial-velocity measurements for non-binary stars, and of the $O-C$ residuals around the computed orbit for binary stars) as a function of the CORAVEL line broadening index Sb (see text). Stars with a cc-dip narrower than the instrumental profile have been assigned $Sb = 0$. Similarly, the jitter has been set to 0 if $\sigma \leq \bar{\epsilon}_1$. Data are from Tables 1–3. Typical error bars on Sb are displayed in the upper left corner. The suspectedly misclassified S stars HD 262427 and BD+22°4385 (Table 3b) have not been plotted. The inset is a zoom of the lower left corner

on Fig. 1. Orbits with a large jitter tend to be associated with giants having large Sb indices. This trend is especially clear among binary S stars, and continues in fact among non-binary S stars (the jitter being then simply the standard deviation of the radial-velocity measurements). Binary ('extrinsic') and non-binary ('intrinsic') S stars actually form a continuous sequence in the (Sb, jitter) diagram of Fig. 1, the transition between extrinsic and intrinsic S stars occurring around $Sb = 5$ km s^{-1}. Intrinsic S stars, with their larger Sb indices ($\gtrsim 5$ km s^{-1}), may thus be expected to be more luminous than extrinsic S stars [$3 \leq Sb$ (km s^{-1}) ≤ 5][1]. This conclusion is confirmed by the luminosities derived from the HIPPARCOS parallaxes (Van Eck et al. 1998). Extrinsic S stars are in turn more luminous than barium stars, with the border case HD 121447 (K7IIIBa5 or S0; Keenan 1950, Ake 1979) having $Sb = 2.8$ km s^{-1}, intermediate between Ba and S stars. HD 60197 (K3Ba5) and BD$-14°2678$ (K0Ba1.5) are two other barium stars with especially large Sb indices, suggestive of a luminosity larger than average for barium stars, though there is no information available in the literature to confirm that suggestion.

Not represented (because accurate ϵ_1 values are lacking) are the two remarkable mild barium stars HD 77247 ($Sb = 5.8$ km s^{-1}) and HD 204075 ($Sb = 4.9$ km s^{-1}) observed at DAO. The latter is indeed known to be a bright giant, with $M_{\rm v} = -1.67$ (Bergeat & Knapik 1997), thus confirming the fact that Sb is a good luminosity indicator for red giants.

The large velocity jitter observed in Mira S stars is a consequence of their complex and variable cc-dips (Barbier et al. 1988; see also Udry et al. 1998a). In some cases however (like

[1] The binary S star HDE 332077, with $Sb = 10.3$ km s^{-1}, is outlying in that respect, as in many others (see Sect. 9.2)

AA Cyg and R Hya), the cc-dips are featureless, broad and very stable. These stars with a comparatively smaller jitter are located on the lower boundary of the region occupied by intrinsic S stars in Fig. 1.

4. Binary frequency

4.1. Strong barium stars

According to Table 2, the frequency of binaries among barium stars with strong Ba indices (Ba3, Ba4 or Ba5) is 35/37, the only stars with constant radial-velocities being HD 19014 and HD 65854. Before coming to a conclusion as to whether binarity is or is not a necessary condition to produce a PRG star, one needs first to assess the barium nature of the constant stars and second, to evaluate the efficiency with which binary stars can be detected with our particular protocol of observations. The latter question is discussed in Sect. 5.

The case of HD 19014 deserves some comments, as its radial velocity appears definitely variable (Table 2b) though with no clear evidence for binary motion. Its only distinctive property is its rather large Sb index of 2.5 km s^{-1}(Fig. 1), suggesting a luminosity larger than average for barium stars. With a radial-velocity standard deviation of 0.5 km s^{-1}, HD 19014 falls right on the (Sb, jitter) correlation observed in Fig. 1, leaving no room for variations due to binary motion.

In the absence of any abundance analysis available for HD 19014, the photometric index $\Delta(38-41)$ defined in the Appendix may be used instead to infer the level of chemical peculiarities of that star. Normal giant stars have $\Delta(38-41) \geq 0$, mild barium stars $-0.1 \leq \Delta(38-41) < 0$, and strong barium stars have $\Delta(38-41) < -0.1$. In that respect, HD 19014 appears to have rather weak peculiarities, if any, as $\Delta(38-41) = -0.01$. Furthermore, in Fig. A.2, it lies in between the loci of normal giants and Ib supergiants, suggesting that the strong barium lines are more likely due to a high luminosity (as inferred from the large Sb index) than to an abundance effect.

HD 65854 is the other strong barium star with no evidence for binary motion (McClure & Woodsworth 1990). Začs (1994) performed a detailed abundance analysis of that star, confirming its barium nature (see also Table 8).

Finally, it has to be noted that BD+38°118 is a triple hierarchical system, with a period ratio $P(ab+c)/P(a+b) = 13$ (Table 2a). At this stage, it is not entirely clear whether the inner pair $a+b$ or the outer pair $ab+c$ is the one responsible for the barium syndrome. Based on the position of the two pairs in the $(e, \log P)$ diagram, it is argued in Sect. 6 that the barium syndrome is more likely to be associated with the wider pair than with the closer one.

4.2. Mild barium stars

The risk of misclassifying a supergiant as a mild barium star is high, since luminosity also strengthens the very lines of BaII and SrII that are often used to identify barium stars (Keenan & Wilson 1977; Smith & Lambert 1987). Excluding the two supergiants obviously misclassified as mild barium stars and listed in Table 1d, the frequency of binary stars among barium stars with mild Ba indices (Ba<1, Ba1 and Ba2) is at least 34/40 (= 85%; Table 1a), and possibly 37/40 (= 93%) when including the suspected small-amplitude binaries HD 18182 and HD 183915 (Table 1b), as well as 56 Peg, an interacting binary system (Schindler et al. 1982). HD 130255 has not been included in the previous statistics, since it has been shown to be a subgiant CH star rather than a barium star (Lambert et al. 1993).

Detailed abundance analyses are available for two among the three constant stars (HD 50843, HD 95345 = 58 Leo and HD 119185). Sneden et al. (1981) find an average overabundance (with respect to solar) of 0.23 dex for the s-process elements in HD 95345. A similar result is obtained by McWilliam (1990). The $\Delta(38-41)$ index of 0.07 is compatible with such a small overabundance level (see the Appendix and Fig. A.1). Začs et al. (1997) find overabundance levels up to 0.4 dex for s-process elements in HD 119185. No detailed analysis is available for HD 50843, but its $\Delta(38-41)$ index of -0.03 is comparable to that of HD 119185 ($\Delta(38-41) = -0.05$), so that s-process overabundances similar to those of HD 119185 may be expected for HD 50843. In summary, all three stars appear to be truly mild barium stars despite the absence of radial-velocity variations.

4.3. S stars

The results of the radial velocity monitoring of S stars are presented in Table 3, which has been subdivided in the following way: (a) S stars for which an orbit or a lower limit on the orbital period is available; (b) S stars with no radial-velocity variations; (c) S stars with radial-velocity variations but no clear evidence for orbital motion; (d) Mira S stars; (e) SC stars.

This partition is motivated by the fact that S stars generally exhibit some radial-velocity jitter very likely due to envelope pulsation, that complicates the search for binaries. This is especially true for Mira S stars and SC stars (see Sect. 3, Fig. 1 and the detailed discussion in Udry et al. 1998a). In these conditions, binary stars are extremely difficult to find among the stars listed in Tables 3d and e. Among these, S UMa may perhaps be binary, but more measurements are needed before a definite statement can be made. The two CS stars with the broadest cc-dips ($Sb > 10$ km s^{-1}), R CMi and RZ Peg, exhibit radial-velocity variations mimicking an orbital motion. These variations are however most probably due to envelope pulsations, since their period is identical to the period of the light variations (see Udry et al. 1998a). An orbital solution has been found for BD−08°1900, but the binary nature of that star is questionable for several reasons, as discussed by Udry et al. (1998a).

The stars listed in Table 3c exhibit radial-velocity variations that cannot satisfactorily be fitted by an orbital solution despite the fact that their jitter is moderate when compared to that of Mira S stars or SC stars.

An interesting difference may be noticed between the S stars with moderate jitter listed in Table 3c and the binary S stars of Table 3a: as already shown in Sect. 3 and Fig. 1, binary S stars are

restricted to the range $2.8 \lesssim Sb$ (km s^{-1}) $\lesssim 5$, whereas Mira, SC and non-binary S stars generally have $Sb \gtrsim 4.5$ km s^{-1} (BD-21°2601, with $Sb = 3.4$ km s^{-1}, is the only exception but since it lacks Tc, it is likely *not* an intrinsic S star). In Sect. 3, it was argued that this separation reflects a difference in the average luminosities of these two groups of S stars (Eq. 1), as confirmed since by Van Eck et al. (1998). This is well in line with the conclusion of previous studies (e.g. Brown et al. 1990; Johnson 1992; Jorissen et al. 1993) that two distinct families, having a very different evolution history, are found among S stars. This 'binary paradigm' states that all Tc-poor S stars should be binaries, being the cool descendants of the barium stars, whereas Tc-rich S stars are genuine thermally-pulsing AGB stars and ought not be binaries. The data presented in Table 3 largely confirm that paradigm, since all Tc-poor S stars (with the only exceptions of HD 189581 and BD-21°2601) are binary stars. The presence of Tc-rich S stars among the binary stars, although allowed in principle, is limited to HD 63733, HD 170970 and o^1 Ori. As argued by Jorissen et al. (1993), the presence of Tc in the former two stars is even questionable, since they fall on the boundary between Tc-rich and Tc-poor stars according to the criterion of Smith & Lambert (1988). The absence of infrared excesses (Jorissen et al. 1993) and their small Sb indices (Fig. 1, where HD 63733 and HD 170970 are flagged as 'Tc doubtful') lend support to their extrinsic nature. o^1 Ori is a very special case, as it shares the properties of extrinsic (in having a WD companion; Ake & Johnson 1988) and intrinsic (in having Tc) S stars. It may be an extrinsic S stars starting its ascent on the thermally-pulsing AGB.

Finally, it should be noted that two S stars with constant radial velocities (Table 3b) were found. The absence of any detectable jitter and their small Sb index are, however, quite unusual for S stars. We therefore suspect that these stars may have been misclassified as S stars. This suspicion appears justified at least for HD 262427, which is listed as S? in the discovery paper of Perraud (1959).

4.4. Tc-poor carbon stars

In their extensive study of Tc in late-type stars, Little et al. (1987) list only 3 carbon stars lacking Tc lines (X Cnc, SS Vir and UU Aur). They might possibly be the analogs of the extrinsic, Tc-poor S stars. If so, they should be binary stars. The results of their CORAVEL monitoring is presented in Table 4, with no clear evidence for binary motion, except perhaps in the case of X Cnc. The large jitter exhibited by these stars (especially SS Vir) is reminiscent of the situation encountered for SC stars, and like them, the Tc-poor C stars have large $B-V$ indices (≥ 3.0).

5. Incompleteness study

5.1. General principles

In order to evaluate the real frequency of binary stars within a given stellar sample, it is of key importance to properly evaluate the efficiency with which binary systems can be detected. That detection efficiency not only depends upon *internal* factors set by the protocol of observations (internal velocity error, sampling and time span of the observations), but also upon *external* factors related to the orbital properties of the binary systems [through the distributions of periods P, eccentricities e, and ratios $Q = M_2^3/(M_1+M_2)^2$], or to their orientation with respect to the line of sight (through the inclinations i and longitudes of periastron ω), or with respect to the time sampling (through the epochs T of passage at periastron).

A Monte-Carlo simulation of our ability to detect binary stars has therefore been performed following the guidelines described by Duquennoy & Mayor (1991). First, N binary systems (where N is the number of stars in the observed sample being tested) are generated by drawing T_j and ω_j ($1 \leq j \leq N$) from uniform random distributions, i_j from a $\sin i$ probability distribution (implying random orientation of the orbital poles on the sky), and P_j, e_j and Q_j from their observed distributions extrapolated in several different ways (see Sect. 5.2).

The synthetic binary j is then attributed the line-width index Sb_j of the jth star in the real sample, and similarly a set of observation dates $t_{j,k}$ ($1 \leq k \leq n_j^{\rm obs}$, $n_j^{\rm obs}$ being the number of observations of the real star j) and a set of internal velocity errors $\epsilon_{j,k}^{\rm int}$. The intrinsic radial-velocity jitter observed for S stars (and, to a much lesser extent, for barium stars; see Fig. 1 and Sect. 3) has to be included in the simulation. To that purpose, a parabolic fit to the trend observed in Fig. 1 has been used to associate a radial-velocity jitter $\epsilon_j^{\rm jit}$ to the selected line width Sb_j. Synthetic velocities $V_{j,k}$ are then computed for the observation dates $t_{j,k}$ from the orbital elements, with an added error drawn from a gaussian distribution of standard deviation $\epsilon_j = [(\overline{\epsilon_j^{\rm int}})^2 + (\epsilon_j^{\rm jit})^2]^{1/2}$, $\overline{\epsilon_j^{\rm int}}$ being the average internal error on one measurement of star j. The few stars measured by other authors[2] have been attributed sets of observation dates, internal velocity errors, line-width indices and jitter from stars of our sample having comparable orbital elements.

Finally, the binary star j is flagged as detected if $P_\nu(\chi_j^2) < 0.01$, where $P_\nu(\chi^2)$ is the χ^2 probability function with $\nu = n_j^{\rm obs} - 1$ degrees of freedom, and $\chi_j^2 = (n_j^{\rm obs}-1)(\sigma_j/\epsilon_j)^2$, σ_j being the unbiased dispersion of the $n_j^{\rm obs}$ synthetic velocities of star j. The detection rate is then $N_{\rm bin}/N$, where $N_{\rm bin}$ is the number of stars with $P_\nu(\chi_j^2) < 0.01$.

This procedure is repeated until 100 sets of N stars have been generated, which is sufficient for the *average* detection rate to reach an asymptotic value. The above method has been applied separately for the sample of 37 barium stars with strong anomalies, of 40 mild barium stars and of 28 S stars with $Sb < 5$ km s^{-1} (referred to as non-Mira S stars in the following). This particular choice for the Sb threshold is motivated by the fact that on Fig. 1, Tc-poor S stars (that are expected to belong to binary systems) are restricted to $Sb < 5$ km s^{-1}. The method has not been applied to Mira S stars because of the uncertain (and probably large) radial-velocity jitter affecting these stars (Sects. 3, 5.3 and Fig. 1).

[2] HD 165141 has not been included in the incompleteness study described in this section, because it was added to Table 1a later on

5.2. Detection rates for specific P, e and Q distributions

The main difficulty of the Monte-Carlo method outlined in Sect. 5.1 is that the *real* distributions of period, eccentricity and Q are not completely known, since the very detection biases we want to evaluate render the *observed* distributions incomplete. Different choices have therefore been made on how to complete the observed distributions, and the sensitivity of the estimated binary detection rates on these choices is evaluated *a posteriori*.

The distribution of ratios Q is likely to have little impact on the detection biases. Therefore, the observed distribution as derived in Sect. 9 has been adopted. Three different cases are considered for the period and eccentricity distributions, as follows:

(i) Uniform distribution in the $(e, \log P)$ diagram

Fig. 2 shows the curves of iso-probability detection for strong barium, mild barium and non-Mira S stars in the $(e, \log P)$ plane. To derive these probabilities, the $(e, \log P)$ plane has been uniformly covered by a mesh of 480 points, which is equivalent to adopting uniform $\log P$ and e distributions. For each of these mesh points, $100N$ (i.e. about 3000) synthetic binaries have been generated as indicated above, in order that the detection probability be mainly set by P and e rather than i, T and ω. As seen on Fig. 2, the detection probability drops tremendously for $P \gtrsim 8000$ d, because of the finite timespan of the observations, which started in 1985 for most strong barium stars, and in 1986 for most mild barium and S stars. For S stars, the intrinsic jitter affecting their radial velocities also contributes to lower the detection rate.

(ii) Observed P and e distributions

In this case, the observed P and e distributions are assumed to represent the *real* distributions, as if there were no systems with periods longer or eccentricities larger than those currently detected in the real samples. This is a conservative choice that allows one to estimate the *maximum* detection rate. With this crude hypothesis, an unfavorable spatial or temporal orientation of the binary system is the only possible cause of non-detection. Eccentricities and periods of the synthetic binaries were drawn in accordance with their observed distribution in the $(e, \log P)$ diagram, using the rejection method described by Press et al. (1992).

The binary detection rates obtained for the three samples under these hypotheses are listed in Table 6 under item Monte-Carlo (ii).

(iii) Extrapolated P and e distributions

In this last case, the real period distribution is assumed to be identical to the observed distribution at short periods. Its long-period tail includes the $N_{\rm no-P}$ stars having no orbital period currently available (i.e. stars with only a lower limit available on P, or even stars with constant radial velocities) but assumed to be very long-period binaries. More precisely, the $N_{\rm no-P}$ stars are uniformly redistributed over the period bins ranging from $P_{\rm inf}$ to 20000 d, where $P_{\rm inf}$ is the first period bin containing a star from the $N_{\rm no-P}$ subsample. Eccentricities are supposed to be uniformly distributed under the curve $e = (\log P - 1)^2/7$.

The corresponding binary detection rates are listed in Table 6 under item Monte-Carlo (iii).

What are the main causes of non-detection? In the case of mild barium stars for example, the non-detected binaries in simulation (iii) are distributed as follows, in decreasing order of importance: $e > 0.8$ for 47.3%, $P > 10^4$d for 32.7%, $-\pi/10 < \omega (\mathrm{mod} \pi) < \pi/10$ for 20.7% (because the radial-velocity curve remains very flat over a large fraction of the orbital cycle around apastron), $\sin i < 0.1$ for 4.5%, and a combination of various less severe conditions for 9.8%. Note that, since a star may belong to more than one of these categories, the sum of the above percentages exceeds 100%. In more practical terms, these numbers translate into 6.6% of the undetected binaries having a radial-velocity semi-amplitude $K < 0.4$ km s^{-1} too small in comparison with the instrumental accuracy, while 37.8% remained undetected because of an incomplete phase coverage ($\Delta t < P/4$) and 26.6% because the number of measurements is too small (< 8).

5.3. Discussion

The detection rates obtained for the various cases considered in Sect. 5.2 are summarized in Table 6, where they are compared with the observed rates.

If binarity were not the rule among barium stars, the observed rates of binaries would be significantly lower than the predicted ones. Here on the contrary, there is a good agreement between the Monte-Carlo predictions and the observed binary rates among mild and strong Ba stars. One may therefore conclude that *binarity is a necessary condition to produce chemically-peculiar red giants like mild and strong Ba stars*. The agreement is slightly better for the Monte-Carlo simulation (iii) extrapolating the period distribution up to 20000 d. The few barium stars with undetected radial-velocity variations are thus likely binaries with very long periods or with unfavourably-oriented orbits.

The situation is more tricky for S stars. The application of the Monte-Carlo method to the *whole* sample of S stars is hampered by our ignorance of the exact amount of jitter in the radial velocities of Mira stars with large Sb indices (see Fig. 1). Therefore the Monte-Carlo simulation cannot be used to evaluate the rate of binaries among the whole sample of S stars (as we did for barium stars). The problem is less severe for S stars with $Sb < 5$ km s^{-1}, where the jitter is smaller (< 1 km s^{-1}) and may be estimated with more confidence. Moreover, the fact that Tc-poor S stars (i.e. extrinsic S stars suspected of belonging to binary systems) appear to be restricted to $Sb < 5$ km s^{-1} provides an independent justification for applying the Monte-Carlo simulation to that subsample. The observed binary rate for S stars with $Sb < 5$ km s^{-1} is close to the one predicted with the extrapolated P and e distributions (case iii in Table 6). This result is thus consistent with the hypothesis that all S stars with $Sb < 5$ km s^{-1} are members of binary systems [Note that,

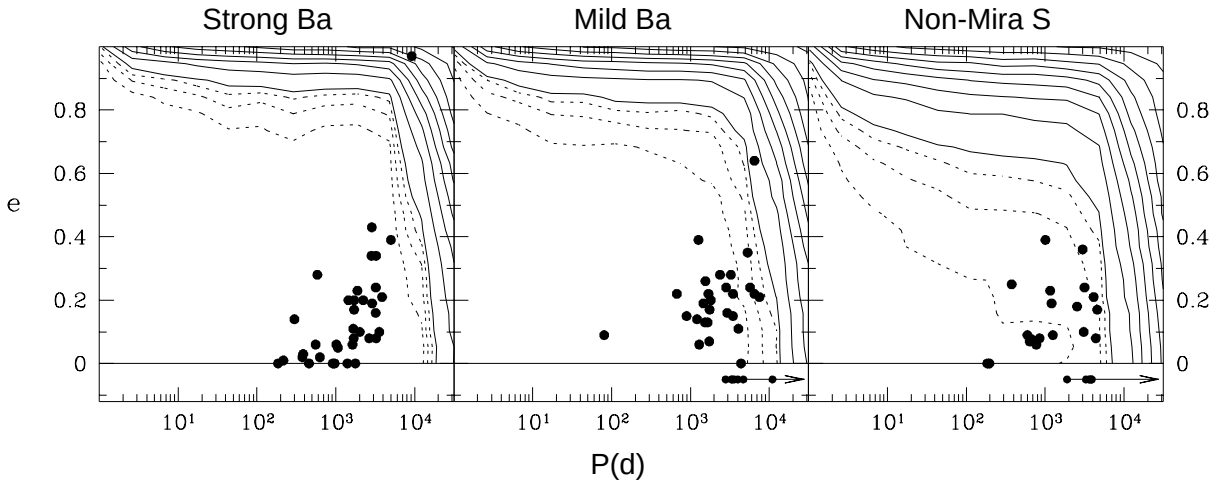

Fig. 2. The iso-probability curves in the $(e, \log P)$ plane for detecting binary systems among strong barium, mild barium and non-Mira S stars. The dotted curves correspond to detection probabilities of 97.5%, 95% and 92.5% (decreasing towards the upper right corner), and the solid curves to probabilities of 90%, 80%, 70%,... In the lower part of each diagram are represented binary stars for which only a lower limit is available on the period

Table 6. Comparison of the simulated and observed binary detection rates for strong barium stars, mild barium stars and non-Mira S stars ($Sb < 5$ km s^{-1}). The quoted uncertainty corresponds to the standard deviation of the detection rates for the 100 stochastically independent sets generated

	strong Ba	mild Ba	S ($Sb < 5$ km s^{-1})
Observed	94.6% = 35/37	85.0% = 34/40 to 92.5% = 37/40	85.7% = 24/28
Monte-Carlo (ii)	$97.9 \pm 3.0\%$ =$(36.2 \pm 1.1)/37$	$93.0 \pm 5.0\%$ =$(37.2 \pm 2.0)/40$	$96.8 \pm 4.0\%$ =$(27.1 \pm 1.1)/28$
Monte-Carlo (iii)	$95.7 \pm 4.0\%$ =$(35.4 \pm 1.5)/37$	$89.4 \pm 6.0\%$ =$(35.8 \pm 2.4)/40$	$89.5 \pm 6.0\%$ =$(25.0 \pm 1.5)/28$

for S stars, the case (iii) predictions have to be preferred over the case (ii) ones, since the period distribution of S stars is most probably incomplete at large periods, due to a more limited time coverage than in the case of barium stars]. However, this agreement should not be overinterpreted, as the $Sb < 5$ km s^{-1} limit between extrinsic and intrinsic S stars may be somewhat fuzzy.

Are there binaries in our sample of intrinsic S stars? For these stars, the intrinsic jitter may possibly induce variations of the same order of magnitude as those caused by binarity, and thus renders the detection of possible binaries very delicate. However, several arguments indicate that binary stars are probably not very frequent among the intrinsic S stars of our sample. The upper panel of Fig. 3 shows the distribution of the radial-velocities standard deviation $\sigma(V_r)$ *predicted* by the Monte-Carlo simulation for a sample of binary stars having orbital parameters matching those of the binary S stars, and with an intrinsic jitter of 1 km s^{-1}. As expected, the *observed* $\sigma(V_r)$ distribution for binary S stars (middle panel of Fig. 3) matches the simulated distribution (allowing for large statistical fluctuations due to the small number of stars observed). On the contrary, the observed $\sigma(V_r)$ distribution for Mira S stars (lower panel of Fig. 3) differs markedly from that of binary S stars, since the former distribution peaks at $\sigma(V_r) \sim 1.5$ km s^{-1} and is rapidly falling off at larger $\sigma(V_r)$. The paucity of Mira S stars with $2 \leq \sigma(V_r) \leq 6$ km s^{-1} must therefore reflect the low percentage of binaries among this group. The minimum value of the jitter (1 km s^{-1}) adopted in the simulation is a conservative choice; a larger jitter would shift the simulated $\sigma(V_r)$ distribution (upper panel) towards larger $\sigma(V_r)$ values, thus strengthening the above conclusion.

Although binarity is not required to produce intrinsic S stars and is indeed not frequent in the sample considered in this paper, binary stars may nevertheless exist among them as in any class of stars. A few intrinsic S stars with main sequence companions are known, from the composite nature of their spectrum at minimum light. They include T Sgr, W Aql, WY Cas (Herbig 1965; Culver & Ianna 1975), and possibly S Lyr (Merrill 1956), as well as the close visual binary π^1 Gru (Feast 1953). A Tc-rich S star with a WD companion is also known (o^1 Ori; Ake & Johnson 1988).

6. The $(e, \log P)$ diagram

The $(e, \log P)$ diagram is a very useful tool to study binary evolution, as the various processes modifying the orbital pa-

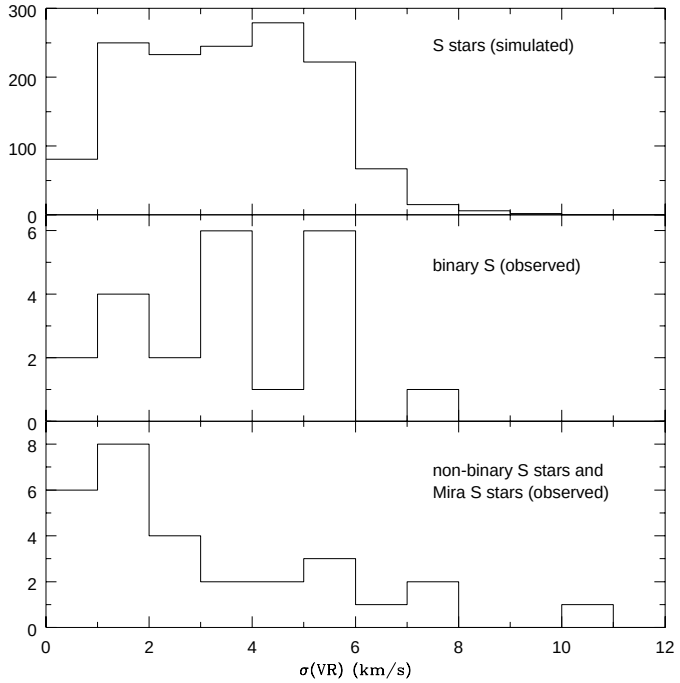

Fig. 3. The *simulated* $\sigma(V_r)$ distribution for binary S stars (upper panel), and the *observed* distribution for real S stars (lower two panels). HD 191589 and HD 332077, the two binary S stars with very discrepant mass functions, lie outside the boundaries of the middle panel, with $\sigma(V_r)$=14.4 and 18.5 km s^{-1} respectively

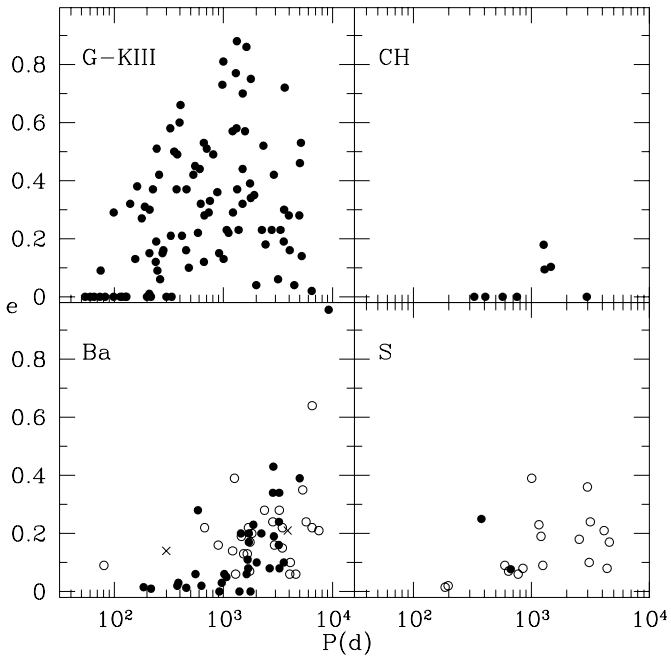

Fig. 4. The $(e, \log P)$ diagram for various samples of red giant stars:
Lower left panel: Barium stars. Mild (Ba<1 – Ba2, from Table 1a) and strong (Ba3 – Ba5, from Table 2a) barium stars are represented by open and filled circles, respectively. The crosses identify the two pairs of the triple hierarchical system BD+38°118;
Upper left panel: Binaries involving G and K giants in open clusters (Mermilliod 1996);
Upper right panel: CH stars (McClure & Woodsworth 1990);
Lower right panel: S stars from Table 3a (Note that HD 121447, the border case between barium and S stars, has been included in both samples). The filled circles correspond to HD 191589 and HD 332077, two S stars with unusually large mass functions (see Sect. 9)

rameters in the course of the evolution (like tidal interaction, RLOF or wind accretion) imprint distinctive signatures on the $(e, \log P)$ diagram (see the various papers in *Binaries as tracers of stellar formation*, edited by Duquennoy & Mayor 1992). The $(e, \log P)$ diagram for various classes of red giants of interest here is displayed in Fig. 4.

The sample of G and K giants from open clusters presented in Fig. 4 (from Mermilliod 1996) will be used as a reference sample to which the binaries involving PRG stars may be compared. A striking feature of this $(e, \log P)$ diagram is the relative paucity of systems with $e < 0.1$ and orbital periods longer than 350 d. A similar lack of circular systems is observed among binary systems involving solar-type main-sequence primaries (Duquennoy & Mayor 1991; Duquennoy et al. 1992), the threshold period (10 d) being much shorter in this case. On the contrary, many systems with periods shorter than this threshold have circular orbits.

Both features are the result of physical processes that operated in the former history of these systems. Tidal effects on the more evolved component nearly filling its Roche lobe are responsible for the circularization of the closest binaries in a given (coeval) sample. The threshold period is then set by the largest radius reached by the more evolved component in its former evolution (Duquennoy et al. 1992; Mermilliod & Mayor 1996). The lack of circular systems above the tidal circularization threshold has been interpreted as an indication that binary systems form in eccentric orbits. A theoretical support to this hypothesis is provided by Lubow & Artymowicz (1992). These authors show that the interaction betwen the young binary system and a circumbinary disk containing proto-stellar residual material may increase a moderate initial eccentricity, thus giving rise to the observed lack of circular orbits among unevolved systems.

The $(e, \log P)$ diagram of barium stars is markedly different from that of cluster giants, for (i) barium stars nearly fill the low-eccentricity gap observed among unevolved binaries[3], (ii) the minimum and maximum periods for a circular orbit are $P_1 \sim 200$ d and $P_2 \sim 4400$ d, respectively, among barium stars, as compared to 50 and 350 d for cluster giants, and (iii) at a given orbital period, the maximum eccentricity found among barium systems is much smaller than for cluster giants. Still, it is important to note that quite large eccentricities ($e \sim 0.97$, HD 123949) are found among barium stars, yet at large periods ($P \sim 9200$ d). The $(e, \log P)$ diagrams of S and CH stars, and

[3] The newly derived orbits for barium systems were never forced to be circular, even though the criterion of Lucy & Sweeney (1971) may indicate that the data is compatible with the hypothesis $e = 0$ at the 5% level. Given the general appearance of the $(e, \log P)$ diagram (Fig. 4), there is no physical reason not to accept small albeit non-zero eccentricities

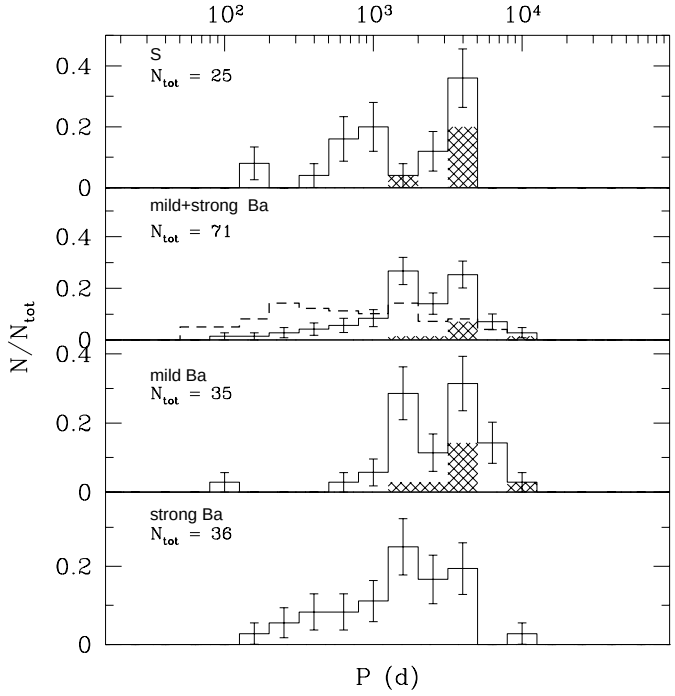

Fig. 5. Period distributions for various families of PRG stars. Shaded regions in the histograms denote systems with only a lower limit available on the orbital period. For comparison, the thick dashed line in the mild+strong Ba panel provides the period distribution for the sample of normal giants in open clusters (Mermilliod 1996; see Fig. 4). The error bars on the histograms correspond to the statistical error expected for a Poisson distribution

their threshold periods P_1 and P_2 in particular, are very similar to those of barium stars.

The differences between the $(e, \log P)$ diagrams of PRG and cluster binaries reflect the fact that the orbits of PRG systems have been shaped by the mass-transfer process responsible for their chemical peculiarities, whereas most of the cluster binaries are probably pre-mass transfer binaries. The $(e, \log P)$ diagram of PRG stars may also have been altered to some extent by tidal effects occurring in more recent phases (e.g., when low-mass barium stars currently in the clump evolved up the RGB), thus complicating its interpretation in terms of mass-transfer only (see Sect. 7). Detailed models of binary evolution are therefore required to fully interpret the $(e, \log P)$ diagram of PRG stars. They are deferred to a forthcoming paper.

Two barium stars deserve some comments. As already indicated in Sect. 4.1, BD+38°118 is a triple system. The large eccentricity ($e = 0.14$) of the inner pair ($P = 300$ d) may therefore not be representative of barium systems and should probably not be regarded as a constraint on the mass-transfer process that shaped the barium-star orbits. Mazeh & Shaham (1979) and Mazeh (1990) have shown that, in a triple system, the dynamical interaction of the inner binary with the third body prevents the total circularization of the inner orbit. However, the oscillation of the eccentricity of the inner binary obtained in the cases considered by these authors has an amplitude (of the order of 0.05) much smaller than the current eccentricity of BD+38°118. It is not clear therefore whether such a dynamical interaction in a triple system may be responsible for the large eccentricity of the inner pair in BD+38°118. Another possibility is that the mass transfer responsible for the barium syndrome actually originated from the distant third companion, whereas the inner pair consisting of the barium giant and a low-mass main sequence companion has orbital elements typical of unevolved systems like those involving giants in clusters. The mass functions of the two pairs are similar (see Sect. 9) and do not contradict the above statement, although they cannot be used to confirm it either.

Another remarkable system is HD 77247, with $P = 80.5$ d and $e = 0.09 \pm 0.01$. There is no indication whatsoever from the $O - C$ residuals of the orbit of McClure & Woodsworth (1990) that this star may belong to a triple system. Yet its orbit should have been circularized by the tidal processes at work in giants, unless that star is much younger than the cluster giants displayed in Fig. 4 (see Duquennoy et al. 1992). An interesting property in that respect is the fact that the star has anomalously broad spectral lines ($Sb = 5.8$ km s^{-1}; Table 1a), an indication that it is either a luminous G (super)giant or that it is rapidly rotating.

7. Period distributions

The orbital-period distributions of mild barium stars, strong barium stars and S stars are compared in Fig. 5, and their distinctive features are outlined in Table 7. The significance of the two modes identified in the period and eccentricity distributions of strong barium stars may be grasped by considering the Roche radii corresponding to the mode boundaries. Adopting 2.1 $M_\odot$ as the typical mass of strong-barium systems (1.5 + 0.6 $M_\odot$; see Table 9), the $\sim$ 1500 d threshold between the short- and long-period modes translates into $A \sim 700$ $R_\odot$ and $R_{\rm Roche} \sim 200$ $R_\odot$ for the Roche radius around the former AGB companion in its final stage (when its mass amounts to ~ 0.6 $M_\odot$). Since this Roche radius is of the order of AGB radii, the threshold between the short- and long-period modes is probably related to the different mass transfer modes arising in detached and semi-detached binary systems (see Sect. 11). The lower boundary of the short-period mode (~ 200 d) corresponds to $A \sim 180$ $R_\odot$, or $R_{\rm Roche} \sim 85$ $R_\odot$ around the barium star. Since this Roche radius is of the order of radii reached on the RGB, the lower end of the short-period mode is likely altered by tidal circularization or even RLOF occurring as the current barium star evolves on the RGB (see Sect. 12).

The upper period cutoff for strong barium stars (which is meaningful, since the sample is complete) is significantly smaller than that of mild barium stars, as expected in the framework of mass transfer through wind accretion (Boffin & Jorissen 1988; Jorissen & Boffin 1992; Sect. 10). The level of chemical peculiarities of a barium star depends, among other parameters, on the amount of matter transferred onto it. Since that amount may in turn be expected to be smaller in wider (i.e. longer-

Table 7. Summary of the distinctive features of the period distributions of mild and strong barium stars

	Strong Ba	Mild Ba
• short-period mode ($P \lesssim 1500$ d)	$e < 0.08$	no short-period mode (except for the peculiar system HD 77247)
• long-period mode ($P \gtrsim 1500$ d)	mild and strong barium stars in this mode are indistinguishable $e > 0.08$	
• upper-period cutoff	5000 d (except for the special case HD 123949: $P \sim 9200$ d, $e = 0.97$)	> 11000 d

period)[4] systems, it is not surprising that the long-period cutoff is larger for mild barium stars. The period cutoffs observed for strong and mild barium stars (5000 and > 11000 d respectively) therefore put constraints on the efficiency of wind accretion, to be used in future simulations.

More generally, milder chemical peculiarities are expected in longer-period systems. However, the broad overlap between the period distributions of mild and strong barium stars (Fig. 5) suggests that the scatter in a (period, chemical anomaly) diagram will be large. It is therefore likely that other parameters play an important role in controlling the level of chemical peculiarities. That question will be addressed in Sects. 8 and 10.

8. Is there a correlation between barium intensity and orbital period?

The existence of a correlation between the orbital separation (or more precisely, periastron distance) and the level of chemical peculiarities would clearly be of key importance for understanding the mass transfer process at work in the progenitor systems of barium stars. Unfortunately, these quantities are not easily available for our complete sample, as not all stars have been the target of detailed abundance analyses on one hand, and on the other hand, the orbital separations cannot be derived for spectroscopic binaries with one observed spectrum without further assumptions. Therefore, the $(P, \Delta(38-41))$ diagram presented in Fig. 6 has been used instead, since the $\Delta(38-41)$ color index is shown in the Appendix to provide a fairly good measure of the heavy-element overabundances (see Fig. A.1). Although there is a general tendency for longer-period systems to exhibit less severe peculiarities [i.e. larger $\Delta(38-41)$ values], as is generally expected for the wind accretion process (Sect. 10 and Theuns et al. 1996), there is a considerable scatter in the $(P, \Delta(38-41))$ diagram[5].

At any given orbital period, the scatter in $\Delta(38-41)$ is clearly larger than would be expected solely from the scatter in the relation between $\Delta(38-41)$ and [YII/TiII] (Fig. A.1). The dispersion in Fig. 6 is therefore likely to reflect real abundance variations at a given orbital period. To confirm that suspicion, heavy-element abundances have been collected from the literature for the barium stars of our sample, and are listed in Table 8. Fig. 7 presents the relation between the orbital period and [s/Fe], where [s/Fe] = 0.5 ([Y/Fe] + [Nd/Fe]) whenever available. It is unlikely that the large scatter observed in Fig. 7 is due to systematic errors between abundances derived by different authors, as indicated by the comparison of HD 121447 ($P = 185$ d, [s/Fe] = 0.70, $\Delta(38-41) = -0.26$, K7Ba5) and HD 178717 ($P = 2866$ d, [s/Fe] = 0.88, $\Delta(38-41) = -0.20$, K4Ba5), both analyzed by Smith (1984). Despite very different orbital periods, the level of chemical peculiarities in these two stars is similar,

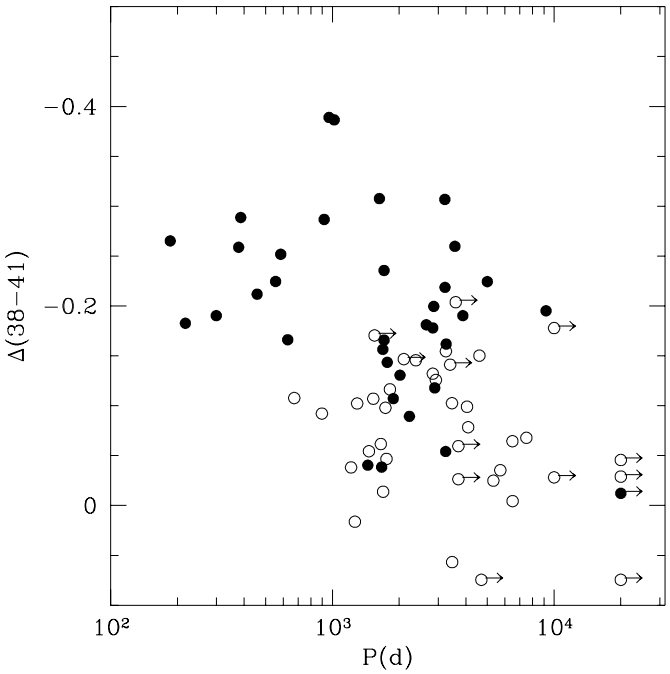

Fig. 6. Orbital period vs $\Delta(38-41)$ index (see Appendix for details), for mild and strong barium stars (represented by open and filled circles, respectively). Arrows indicate that only a lower limit is available for the orbital period. Stars with only marginal evidence for binary motion (very low-amplitude variations, if any; Table 1b) have been arbitrarily assigned a period of 10^4 d, whereas constant stars have been assigned a period of 2 10^4 d, for comparison

[4] It is in fact the periastron distance rather than the orbital period which is the key parameter in this respect. The long period (~ 9200 d) observed for the strong barium star HD 123949 is therefore not relevant, since its very large eccentricity yields a periastron distance much smaller than in systems with $P \sim 5000$ d and smaller eccentricities

[5] The scatter is even more severe if one considers periastron distance instead of orbital period

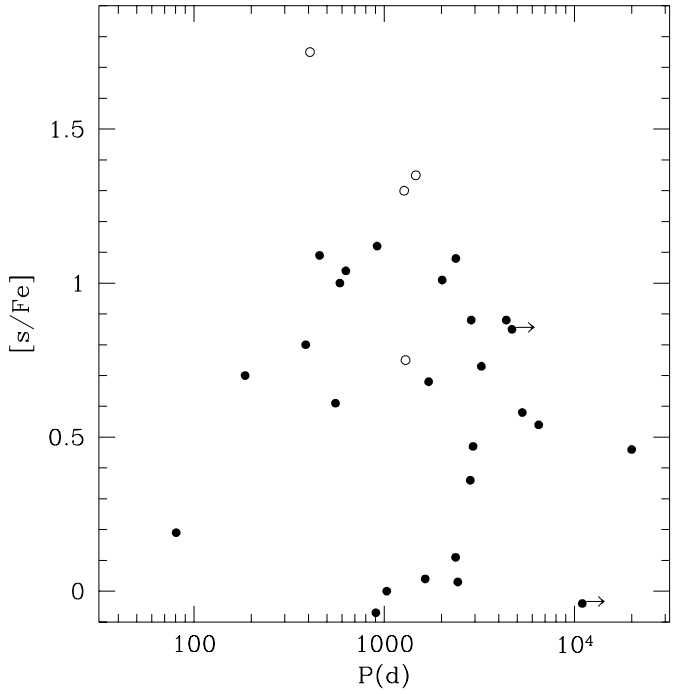

Fig. 7. Orbital period vs heavy-element overabundance [s/Fe] (see Table 8). Filled dots correspond to barium and normal giants in barium-like binary systems, whereas open dots correspond to CH stars. Arrows correspond to lower limits on the orbital period. The constant-velocity star HD 65854 has been arbitrarily assigned a period of 2 10^4 d

as indicated not only by their heavy-element overabundances (Table 8) but also by their fluorine abundance (Jorissen et al. 1992a). Moreover, several giants with *normal* heavy-element abundances, albeit in binary systems with barium-like orbital elements, are also shown on Fig. 7. Their very existence is another clear indication that the orbital separation is not the only parameter controlling the level of chemical peculiarities in barium stars. These barium-like binary systems involving a normal giant are listed in Table 8 and are collected from the catalogue of Boffin et al. (1993), listing all spectroscopic binary systems with a giant component. That catalogue has been searched for systems involving a red giant with normal heavy-element abundances according to McWilliam (1990), and falling in the region $e < 0.1$, $P > 350$ d of the $(e, \log P)$ diagram (Fig. 4). That region of the $(e, \log P)$ diagram is normally not populated by pre-mass-transfer systems, as discussed in Sect. 6, so that the unseen component in these systems may be supposed to be a WD. No direct confirmation for the presence of a WD is however available for HD 33856 and HD 66216. For HD 13611 (=ξ^1 Ceti), Böhm-Vitense & Johnson (1985) reported some UV excess that they attribute to a WD companion, though that statement has subsequently been questioned (Jorissen & Boffin 1992; Fekel et al. 1993). The clearest case of a post-mass-transfer system consisting of a WD and a *normal* red giant is undoubtedly HD 160538 (=DR Dra). Orbital elements ($P = 904$ d, $e = 0.07$) have been obtained by Fekel et al. (1993), along with definite evidence for the presence of a hot WD. An abundance analysis of that star has recently been carried out by Berdyugina (1994), who concludes that HD 160538 is a solar-metallicity giant ([Fe/H] $= -0.05$) with normal Zr, Ba and La abundances.

These counter-examples (especially DR Dra) strongly suggest that *binarity is not a sufficient condition to produce a barium star!* Another condition – like a low metallicity? – seems thus required to form a barium star, and such a hidden parameter may, at least in part, be responsible for the blurred correlation between the orbital period and the intensity of the chemical anomalies. Unfortunately, it is difficult to evaluate the exact influence of metallicity on that correlation, because an homogeneous set of metallicity determinations is lacking for the stars in our sample. Large systematic differences may indeed be present between the metallicity determinations by different authors, as discussed e.g. by Busso et al. (1995). As an illustration, metallicities ranging from -0.45 to +0.13 have been published for HD 46407! The location of CH stars in Fig. 7 nevertheless lends strong support to the idea that metallicity is the hidden parameter controlling the level of chemical peculiarities at a given orbital period, since these low-metallicity stars have the largest [s/Fe] values at any given orbital period. Kovács (1985) also noticed that there is a correlation between [Ba/Fe] and metallicity [Fe/H]: strong barium stars generally have a metallicity lower than mild barium stars (see also the recent compilation of Busso et al. 1995, and North et al. 1994 for a similar finding among barium *dwarfs*). Clayton (1988) provided a theoretical foundation for that empirical finding: if $^{13}\mathrm{C}(\alpha, \mathrm{n})^{16}\mathrm{O}$ is the neutron source responsible for the operation of the s-process, its efficiency in terms of neutron exposure is expected to be larger in a low-metallicity environment. Therefore, barium stars would be easier to produce in a low-metallicity population. That question will be discussed in more details in Sect. 10, since there are obviously other parameters involved (like the dilution factor and the amount of matter transferred from the former AGB companion) whose impact should be evaluated as well.

9. The mass-function distributions

9.1. Barium and CH stars

The cumulative frequency distribution of mass functions $f(M)$ conveys information on the masses of the two components in the binary system, since

$$f(M) = \frac{M_2^3}{(M_1 + M_2)^2} \quad \sin^3 i \equiv Q \sin^3 i, \tag{2}$$

M_1 and M_2 being the masses of the red giant and of its companion, respectively. As shown by Webbink (1986) and McClure & Woodsworth (1990), the $f(M)$ distribution of peculiar red giants like barium and CH stars is very different from that of normal red giants. The PRG distributions are in fact compatible with a narrow range of Q values, convolved with random orbital inclinations. McClure & Woodsworth (1990) obtained $Q = 0.041 \pm 0.010$ $\mathrm{M}_\odot$ for their sample of 16 barium stars, and $Q = 0.095 \pm 0.015$ $\mathrm{M}_\odot$ for CH stars. Such narrow Q distributions are indeed expected if the companions of PRG stars are WD stars with masses spanning a narrow range, as is the

Table 8. Abundances of s-process elements in CH stars, barium stars and normal giant stars belonging to a barium-like binary system. The column labeled 'elements' lists the elements involved in [s/Fe]. Usually [s/Fe] = 0.5 ([Y/Fe] + [Nd/Fe]); YII/TiII in that column means that [s/Fe] corresponds to the [Y/Ti] ratio taken from McWilliam (1990; see Appendix for details). The column labeled 'Ref' provides the reference for the [s/Fe] data, according to the notes at the end of the table. The orbital periods of CH systems are from McClure & Woodsworth (1990)

a. CH stars

HD	HR	Sp. Typ.	P (d)	$\Delta(38-41)$	[s/Fe]	elements	Ref
209621		CH	407		1.75	Y, Nd	7
224959		CH	1273		1.30	Y, Nd	7
198269		CH	1295		0.75	Y, Nd	7
201626		CH	1465		1.35	Y, Nd	7

b. Barium stars

77247		G5 Ba1	80	-	0.19	Y, Nd	3
121447		K7 Ba5	185	-0.26	0.70	Y, Nd	1
CpD $-64^\circ 4333$		K0 Ba4	386	-0.29	0.80	Y	1
46407	2392	K0 Ba3	457	-0.21	1.09	Y, Nd	2
100503		K3 Ba5	554	-0.25	0.61	Y	1
199939		K0 Ba4	585	-0.25	1.03	Y, Nd	3
44896		K3 Ba5	629	-0.17	1.04	Y, Nd	1
92626		K0 Ba5	918	-0.29	1.12	Zr, Nd	2
101013	4474	K0 Ba5	1711	-0.17	0.68	Y, Nd	3
16458	774	K1 Ba5	2018	-0.13	1.01	Y, Nd	1
204075	8204	G5 Ba2	2378	-0.15	1.08	YII/TiII	5
205011		K1 Ba1	2837	-0.13	0.36	Y, Nd	3
178717		K4 Ba5	2866	-0.20	0.88	Y, Nd	1
131670		K1 Ba1	2930	-0.13	0.47	Y, Nd	3
60197		K3 Ba5	3243	-0.05	0.73	Y, Nd	1
196673		K2 Ba2	6500	0.00	-0.19	Zr, Nd	3
199394		G8 Ba1	4606	-0.15	0.88	Y, Nd	3
104979	4608	K0 Ba1	> 4700	0.07	0.85	Y, Nd	4
139195	5802	K1 Ba1	5324	-0.02	0.58	YII/TiII	5
202109	8115	G8 Ba< 1	6489	-0.06	0.54	YII/TiII	5
98839	4392	G7 Ba< 1	> 11000	-	-0.04	Y, Nd	8
65854		K1 Ba3	cst	-	0.46	Y, Nd	3

c. Normal giants in barium-like binary systems

160538		K0III + WD	904	-	-0.07	Zr, Ba, La	6	DR Dra
33856	1698	K0.5III	1031	-	0.00	YII/TiII	5	
13611	649	G8III + WD?	1642	0.07	0.04	YII/TiII	5	ξ^1 Cet
169156	6884	K0III	2374	-	0.11	YII/TiII	5	
66216	3149	K2III	2438	-	0.03	YII/TiII	5	

References:
1: Smith 1984; 2: Kovács 1985; 3: Začs 1994; 4: Tomkin & Lambert 1986; 5: McWilliam 1990; 6: Berdyugina 1994; 7: Vanture (1992); 8: Sneden et al. (1981).

case for field WDs (Reid 1996). On the contrary, since the companions of normal giants in binary systems ought not be WDs, their masses may span a much wider range (the only constraint being then $M_2 \leq M_1$), thus contrasting with the PRG $f(M)$ distributions.

The larger samples considered in this paper make it possible to derive the distributions of Q separately for mild and strong barium stars. These distributions have been extracted from the observed distribution of $f(M)$ by two different methods. In the first method, the observed $f(M)$ distribution is simply compared to simulated distributions assuming random orbital inclinations and gaussian distributions (of mean $\overline{M}_i$ and standard deviation σ_i, $i = 1, 2$) for the masses M_i of the two components. Since $f(M)$ depends upon the masses only through the ratio $Q = M_2^3/(M_1+M_2)^2$, almost equally good fits (expressed in terms of the greatest distance D between the synthetic and observed $f(M)$ distributions) are obtained for different combinations of $\overline{M}_1$ and $\overline{M}_2$, all corresponding to the same value of

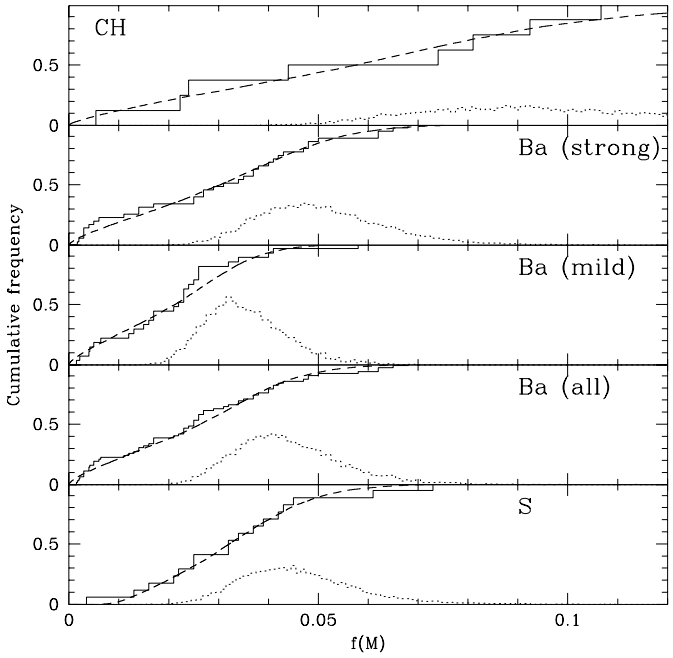

Fig. 8. Comparison of the synthetic (dashed line) and observed (solid line) mass-function distributions for CH stars (top panel, with data from McClure & Woodsworth 1990), strong barium stars (second panel from top, from Table 2a), mild barium stars (third panel from top, from Table 1a), all barium stars (fourth panel from top), and S stars (bottom panel, from Table 3a). For S stars, the synthetic distribution has been constructed by adopting a detection threshold $i > 36^\circ$ to simulate the deficit of systems with small mass functions (see text). The dotted line corresponds to the distribution of Q

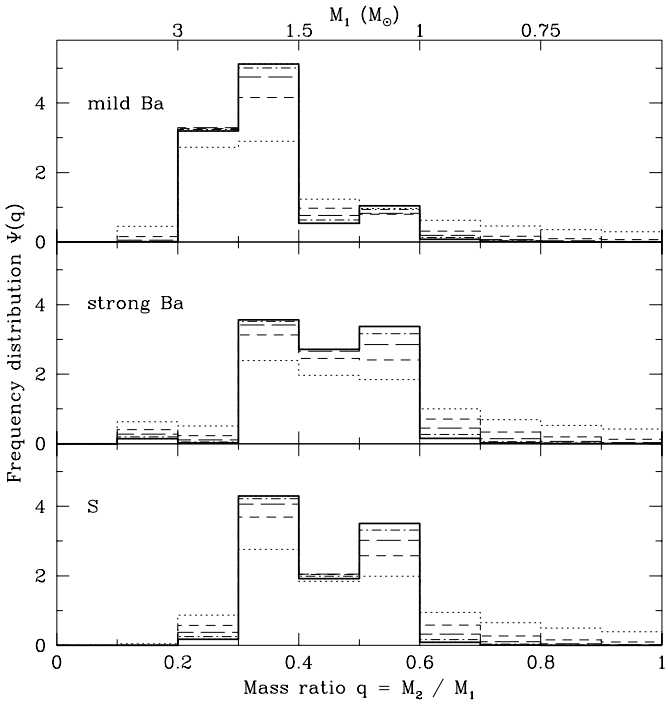

Fig. 9. Distributions of mass ratios $q = M_2/M_1$ extracted from the observed $f(M)$ distributions using the Richardson-Lucy iterative algorithm, for mild barium stars (upper panel), strong barium stars (middle panel) and S stars (lower panel). During the inversion process, M_2 has been fixed at 0.6 $M_\odot$. The corresponding mass M_1 of the giant star can be read from the upper scale. The various lines refer to the distributions obtained after 2 (dotted line), 4 (short-dashed line), 6 (long-dashed line), 8 (dash-dotted line) and 10 (thick line) iterations

Table 9. Average masses $\overline{M}_1$ of the giant star in various PRG families as derived from the cumulative frequency distribution of the mass functions, for two different values of the companion average mass $\overline{M}_2$. N is the number of available orbits

Family	N	$\overline{Q}$	$\overline{M}_1$		Ref
			$\overline{M}_2 = 0.60$	$\overline{M}_2 = 0.67$	
		($M_\odot$)	($M_\odot$)	($M_\odot$)	
CH	8	0.095	0.9	1.1	2
Barium (strong)	36	0.049	1.5	1.9	1
Barium (mild)	27	0.035	1.9	2.3	1
Barium (total)	63	0.043	1.65	2.0	1
S (extrinsic)	17[a]	0.041	1.6	2.0	1

Remark: a: the two peculiar S stars HD 191589 and HDE 332077 were not included (see Sect. 9.2)
References: 1. This work; 2: McClure & Woodsworth (1990)

$\overline{Q}$. The value of $\overline{Q}$ minimizing D for the different PRG families is listed in Table 9. The synthetic and observed $f(M)$ distributions are compared in Fig. 8. The best fits are obtained with $\sigma_1 = 0.2$ $M_\odot$ and $\sigma_2 = 0.04$ $M_\odot$.

A similar analysis performed by North et al. (1997) on a sample of *dwarf* barium stars provided the first independent estimate of the average companion mass. Unlike the barium giants, the barium dwarfs offer the possibility to directly derive their masses by fitting evolutionary tracks to their observed surface gravities and effective temperatures. The known distribution of primary masses and the average ratio Q derived from the $f(M)$ distribution then yield an average mass $\overline{M}_2$ of 0.67 ± 0.09 $M_\odot$ for the companion. Assuming that dwarf barium stars, giant barium stars and extrinsic S stars represent successive stages along the same evolutionary path (Sects. 12 and 13), the $\overline{M}_2$ value derived by North et al. (1997) for the companions of dwarf barium stars may be adopted to derive the average mass $\overline{M}_1$ of the giant for the different PRG families listed in Table 9. For comparison, the average mass $\overline{M}_1$ corresponding to $\overline{M}_2 = 0.60$ $M_\odot$ has also been listed.

The second method, described by Cerf & Boffin (1994) and based on the Richardson-Lucy iterative inversion algorithm, fully confirms the above results. Fig. 9 shows the extracted distributions of mass ratios $q = M_2/M_1$ and masses M_1 when M_2 is fixed at 0.6 $M_\odot$.

The $f(M)$ distributions of CH stars, mild barium stars and strong barium stars are clearly distinct, and this difference is reflected in the corresponding average masses $\overline{M}_1$ listed in Table 9. A Kolmogorov-Smirnov test confirms the significance of this difference, since the null hypothesis that the distributions of

mild and strong barium stars are extracted from the same parent population may be rejected with a first kind risk of only 0.6%.

Although the difference in the Q distributions of mild barium stars, strong barium stars and CH stars may equally well result from a difference in the giant or companion masses, the different kinematical properties reported for these families suggest a difference in the respective masses of the *giant* star. The kinematics of CH stars is typical of a halo population (McClure 1984ab and references therein), whereas barium stars belong to a disk population. Moreover, there are several pieces of evidence that mild barium stars belong to a somewhat younger population than strong barium stars. Catchpole et al. (1977; see also Lü 1991) showed that the velocity dispersion of mild barium stars is smaller than that of strong barium stars. From a statistical analysis of the positions of barium stars in the Hertzsprung-Russell diagram based on Hipparcos parallaxes, Mennessier et al. (1997) conclude that mild barium stars are mostly clump giants with a mass in the range 2.5 – 4.5 $M_\odot$, whereas strong barium stars populate the giant branch and have masses in the range 1 – 3 $M_\odot$. These mass estimates are consistent with those derived from the mass-function distributions (Fig. 9).

It may thus be concluded that mild barium stars, strong barium stars and CH stars represent a sequence of increasingly older galactic populations.

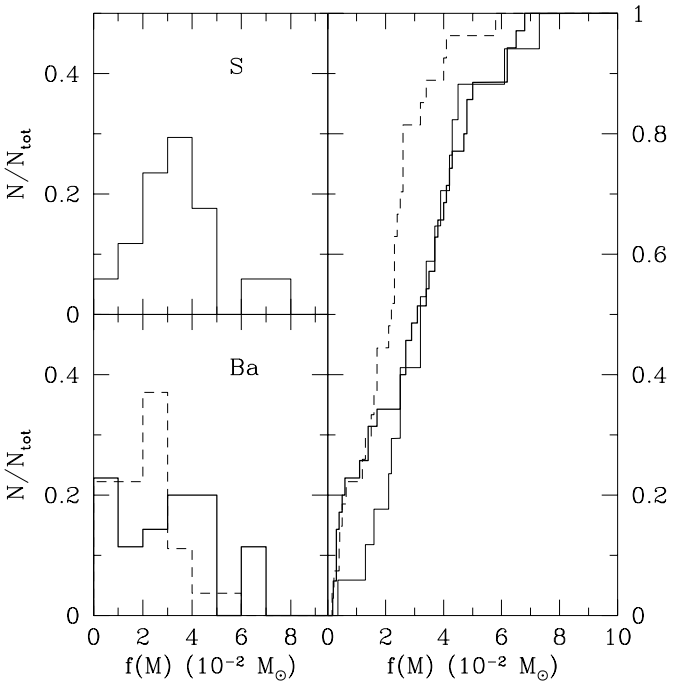

Fig. 10. Comparison of the mass-function distributions of barium stars (thick solid line: strong barium stars; thin dashed line: mild barium stars) and S stars (thin solid line). The mass functions of HD 191589 and HDE 332077 were not included in the comparison

9.2. S stars

Fig. 10 compares the cumulative distributions of mass functions for barium and S stars. Apart from a deficit of systems with small mass functions, the $f(M)$ distribution of S stars is very similar to that of strong barium stars. The deficit of S systems with small mass functions $f(M)$ can probably be attributed to the difficulty of detecting small-amplitude binaries for these stars with a substantial radial-velocity jitter (Sects. 3 and 5.2, and Figs. 1 and 2).

Note that the two S stars HD 191589 and HDE 332077 were not included in the comparison, since they have very discrepant mass functions of 0.395 and 1.25 $M_\odot$, respectively (Table 3a). A-type companions were detected for these stars with the *International Ultraviolet Explorer* (Ake & Johnson 1992; Ake et al. 1992), consistent with their mass functions. From the current radial-velocity data, there is no indication that these systems might be triple. The evolutionary status of these Tc-poor S stars is currently unclear.

10. Mild vs. strong barium stars: entangled effects of orbital dynamics and galactic population

In the previous sections, mild and strong barium stars have been seen to differ in many respects: (i) short-period ($P \lesssim 1500$ d), nearly-circular systems are lacking among mild barium stars, (ii) there is a tendency for systems with longer periods to have milder chemical anomalies, although the large scatter in that relation suggests that some other parameter (like metallicity?) partially controls the level of chemical anomalies, (iii) strong barium stars generally have lower metallicities than mild barium stars, (iv) mild barium stars have smaller mass functions on average, and (v) mild barium stars are kinematically younger than strong barium stars.

The previous facts consistently suggest that mild barium stars belong to a younger, more metal-rich and more massive population than strong barium stars. In this section, we investigate the consequences of this difference in galactic population on the mass-transfer process. For that purpose, the chemical anomalies of mild and strong barium stars are computed using a simple dynamical model, assuming that the former AGB progenitor of the present WD has dumped heavy-element-rich matter onto its companion.

The parameters controlling the intensity of chemical anomalies in barium stars may be easily identified with the aid of the following formula, relating the overabundance factor s of heavy elements in the envelope of the barium star (i.e. the ratio between the abundances after completion of the accretion and dilution processes, and the initial envelope abundances) to their overabundance f in the material accreted from the former AGB star:

$$s = \frac{f\Delta M_{\rm Ba} + M_{\rm Ba,0} - M_{\rm Ba,core}}{\Delta M_{\rm Ba} + M_{\rm Ba,0} - M_{\rm Ba,core}} \equiv f\mathsf{F} + (1-\mathsf{F}), \qquad (3)$$

where F is the dilution factor of the accreted matter $\Delta M_{\rm Ba}$ in the envelope of mass $(M_{\rm Ba,0} - M_{\rm Ba,core} + \Delta M_{\rm Ba})$. Here, $M_{\rm Ba,0}$ and $M_{\rm Ba,core}$ denote the initial total mass and core mass, respectively, of the accreting barium star. The accreted mass $\Delta M_{\rm Ba}$ is computed from the relation

$$\Delta M_{\rm Ba} = \beta(M_{\rm AGB,0} - M_{\rm WD}), \qquad (4)$$

where β corresponds to the fraction of the mass lost by the former AGB star of mass $M_{\rm AGB,0}$ (at the start of the thermally-pulsing phase) that is actually accreted by the barium star. For the sake of simplicity, it is assumed that all cases considered below undergo wind accretion (so that predictions will be restricted to systems with $P \gtrsim 1500$ d, in accordance with the discussion of Sect. 7). The Bondi & Hoyle (1944) prescription will therefore be adopted for computing the accretion efficiency β (see Theuns et al. 1996 for more details):

$$\beta = \frac{\alpha}{A^2}\left(\frac{GM_{\rm Ba}}{v_{\rm w}^2}\right)^2 \frac{1}{[1+(v_{\rm orb}/v_{\rm w})^2]^{3/2}}, \quad (5)$$

or using Kepler's third law:

$$\beta = \alpha\mu^2 \frac{k^4}{[1+k^2]^{1.5}}, \quad (6)$$

where $k \equiv v_{\rm orb}/v_{\rm w}$, $v_{\rm orb}$ and $v_{\rm w}$ being the relative orbital velocity ($2\pi A/P$) and the wind velocity, respectively, G is the gravitational constant, A is the orbital separation, $\mu \equiv M_{\rm Ba}/(M_{\rm AGB}+M_{\rm Ba})$, and α is a scaling parameter. In the above relation, it has been assumed that the wind is highly supersonic. Detailed hydrodynamic simulations (Theuns et al. 1996) have shown that $\alpha \sim 0.05$ in the situation of interest here.

The above relations thus indicate that the following parameters will have some impact on the level of chemical anomalies:
(i) a large orbital separation will result in a small accretion cross section (Eq. 5, valid for a wind-accretion scenario). Note, however, that the functional dependence of β with A is more complicated than the simple explicit A^{-2} factor appearing in Eq. (5), since there is an implicit dependency through the orbital velocity $v_{\rm orb}$;
(ii) a lower mass for the barium star results in a smaller dilution (i.e. larger F). However, the effect is opposite on the accretion cross section (Eq. 5), notwithstanding the implicit dependence through $v_{\rm orb}$;
(iii) a smaller metallicity probably results in larger heavy-element overabundances f in the AGB progenitor (see the discussion at the end of Sect. 8). As low-metallicity giants are expected to have low masses, this effect is strongly coupled with (ii);
(iv) a larger mass for the AGB progenitor results in more mass being lost and thus accreted by the companion; a more massive WD is also produced.

The above qualitative discussion shows that the various relevant parameters are strongly coupled with each other, thus calling for detailed calculations. Because in the framework of the simple wind-accretion model adopted here, the accretion rate depends upon the orbital separation (see Eq. 5), the resulting overabundance s must be computed by taking into account the variation of the orbital separation in the course of the mass transfer process. Neglecting the anisotropy in the mass loss process induced by the accretion, as well as a possible transfer of linear momentum from the wind to the accreting star (see Theuns et al. 1996), the variation of the orbital separation obeys the equation:

$$\frac{\dot{A}}{A} = -\frac{\dot{M}_1+\dot{M}_2}{M_1+M_2}. \quad (7)$$

The amount of accreted matter has been computed by integrating Eqs. (3)–(7) using a Runge-Kutta scheme, starting with $M_{\rm AGB,0}$ equal to $M_{\rm Ba}$ (the present mass of the barium star), and integrating till $M_{\rm AGB} = M_{\rm WD} = 0.67$ M$_\odot$ (see Table 9). This initial condition ensures that the AGB star was initially slightly more massive than the barium star, and evolved faster. The amount of mass accreted thus represents a lower limit, as the AGB star might have been more massive initially.

Different combinations of paramaters have been considered, so as to evaluate the relative importance of items (i), (ii) and (iii) listed above. To evaluate the impact of the population difference between strong and mild barium stars (see Table 9), cases with $M_{\rm Ba} = 1.8$ (mimicking strong barium stars, and labelled L in the following) and 2.4 M$_\odot$ (mimicking mild barium stars, and labelled H in the following) have been considered. To evaluate the impact of metallicity (item iii), surface s-process overabundances f of 130 and 40 in low- and high-metallicity AGB stars, respectively, were considered (labelled l and h, respectively, in the following). The overabundance s of heavy elements for cases Hh, Lh and Ll is shown on Fig. 11 as a function of the *final* orbital period P (for $P \gtrsim 1500$ d, as shorter final periods most probably involve RLOF, not adequately described by the present scheme). The overabundance f of heavy elements in the accreted matter is clearly of utmost importance in controlling the pollution level s. In particular, it is clear that different giant masses (Table 9) cannot explain the different pollution levels of mild and strong barium stars (compare cases Lh and Hh on Fig. 11). The respective overabundances s obtained in cases Hh and Lh are even opposite to what is expected from the observations, since the more massive mild barium stars (Hh) would be *more polluted* than the strong barium stars (Lh) for a given f! This contradiction results from the fact that more mass was allowed to be exchanged in the 'mild barium' systems because the AGB progenitor was supposed to be more massive in the more massive mild barium systems than in the strong barium systems (see above).

The mass of the AGB progenitor sensitively controls both the amount of mass that can be exchanged (thus fixing the pollution level) and the mass of the WD (thus fixing Q). It offers therefore a way to link the differences in pollution levels and mass functions that are observed in mild and strong barium stars. However, because that explanation cannot account for the kinematic differences observed between mild and strong barium stars (Sect. 9.1), we favour an explanation in terms of a difference in the f values characterizing the matter accreted by the barium stars belonging to the H and L populations having different metallicities. We find that, with the choice $f = 40$ and 130, the difference between mild and strong barium stars is largely one of population, strong barium stars belonging almost exclusively to a low-mass low-metallicity population characterized by a large value of f (represented by case Ll). Some merging between the H and L populations inevitably occurs for mild barium stars, however, since they contain all stars with $0.2 \lesssim \log s \lesssim 0.5$ (see Fig. 11). This prediction receives some support from the mass distribution of mild barium stars presented in Fig. 9. Although mild barium stars are dominated by

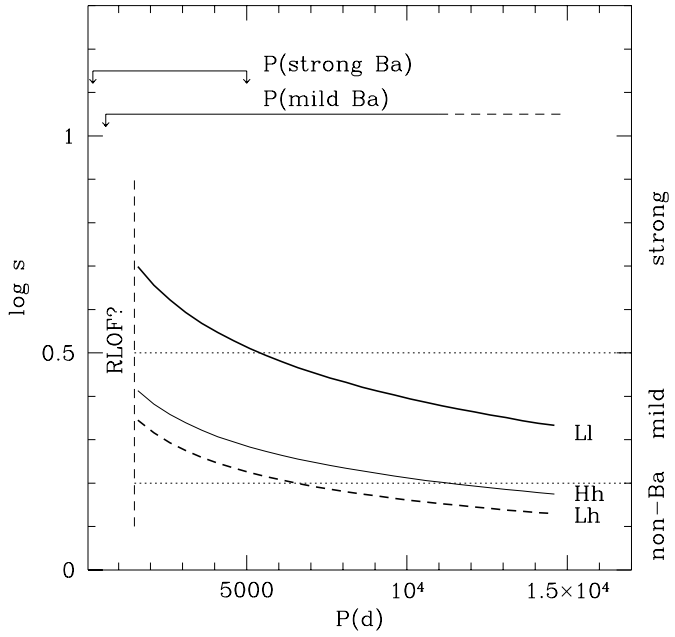

Fig. 11. Schematic predictions of the wind-accretion scenario [Eqs. (3) – (7)] for the cases Ll, Lh and Hh defined in the text. The dotted lines mark the (somewhat arbitrary) separation between strong, mild and non-barium stars. The range in periods spanned by mild and strong barium stars is represented by the horizontal lines in the upper part of the figure

high-mass objects ($M_1 \sim 1.5$ – 3 $M_\odot$, corresponding to the H population in the above simulations), there is a small tail of less massive objects which suggests that mild barium stars are indeed a mixture of populations H and L.

The above values of f appear plausible in view of the s-process overabundances reported by Utsumi (1985) and Kipper et al. (1996) in N-type carbon stars, supposed to be representative of the former AGB mass-losing star in the barium systems. However, the parameter f is admittedly not very tightly constrained by our simple model. It is therefore encouraging that the value of f chosen to reproduce the upper period cutoff of strong barium stars (in case Ll) predicts that mild barium stars can be produced in systems with periods up to a few 10^4 d which is consistent with the longest periods observed among mild barium stars (Sect. 5.3).

Another argument related to CH stars lends strong support to the idea that f increases in low-metallicity populations, and is the principal factor controlling the pollution levels of PRG stars. Although the periods of CH stars span the same range as those of barium stars (Fig. 4), their heavy-element overabundances at a given period are generally larger than those of barium stars (Fig. 7 and Table 8). Applying the method described above to CH stars, it is found that values of f of the order of 300 at least are required to account for the observed overabundance levels s. The operation of the s-process must therefore have been very efficient in the low-metallicity AGB star responsible for the pollution of the CH star envelope (see also the discussion in Sect. 8). There is a very distinct property of the heavy-element abundance distribution observed in CH stars that confirms this fact. Heavy s-process elements ('hs') like Ba are comparatively more overabundant than light s-process elements ('ls') like Y, with [hs/ls]≥ 0.4 (Vanture 1992). This situation is only encountered when the neutron exposure τ which characterizes the efficiency of the s-process reaches values as large as 1 mb^{-1} (Vanture 1992). Such values lead to overabundances of heavy s-elements that are comparatively larger than for smaller τ (e.g. Fig. 5 of Busso et al. 1995), in agreement with the above requirement for large f values in CH systems.

11. Short-period Ba systems and the question of RLOF

The mass-transfer model [Eqs. (3) – (7)] used in Sect. 10 to evaluate the respective importance of the various parameters entering the problem is extremely schematic. In particular, it assumes that mass transfer occurs through wind accretion. That assumption is clearly not valid at the short end of the period distribution, where Roche lobe overflow (RLOF) enters the stage (see Sect. 7; Han et al. 1995; Jorissen et al. 1995). In fact, the wind-accretion scenario considered in Sect. 10 predicts that the system widens as it loses mass. For systems with periods shorter than ~ 1500 d, that prediction is clearly incompatible with the requirement that the system remained detached during mass transfer (see also the discussion in Jorissen et al. 1995). Adopting for instance $M_{\rm AGB} = 0.6$ $M_\odot$, $M_{\rm Ba} = 1.5$ $M_\odot$ and $P = 1500$ d yields a Roche radius of about 200 $R_\odot$, much smaller than typical radii of ~ 500 $R_\odot$ observed for cool ($T_{\rm eff} \sim 2200$ K) Mira stars (e.g. van Belle et al. 1996). In such circumstances, it seems unavoidable that at least the shortest-period systems among barium stars result from RLOF. That conclusion is puzzling, however, in view of the catastrophic outcome generally associated with RLOF when the mass-losing star is the more massive one and has a deep convective envelope as is the case for AGB stars. Mass transfer then occurs on a dynamical time scale ('unstable case C' mass transfer), and leads, via a common envelope stage, to the formation of cataclysmic variable stars with orbital periods of a few hours (e.g. Meyer & Meyer-Hofmeister 1979; de Kool 1992; Iben & Tutukov 1993; Ritter 1996). Barium stars must somehow have avoided this evolutionary channel. In the remainder of this section, several ways out of this channel are briefly suggested.

First, it is possible that the common envelope phase developing during unstable case C mass transfer does not lead to a dramatic orbital shrinkage if mechanisms internal to the AGB star reduce the effective binding energy of its envelope (like the recombination energy in the hydrogen and helium ionization zones, excitation of non-radial pulsation modes, shock-heating, dust-driven winds...; Iben & Livio 1993). In those cases, not so much energy ought to be extracted from the orbit to expell the common envelope, thus reducing (and even perhaps suppressing) the orbital decay. Due consideration of the thermal energy of the AGB envelope reduces its effective binding energy and the orbital shrinkage associated with a common-envelope phase is therefore limited. Han et al. (1995) have shown that barium

systems like HD 77247 with periods as short as 80 d may form under such circumstances.

Second, the dynamical instability associated with case C mass transfer is suppressed when the mass-losing star is *less massive* than its companion (Pastetter & Ritter 1989), with $q < q_{\rm crit} < 1$, where $q = M_{\rm AGB}/M_{\rm Ba}$ and $q_{\rm crit}$ is given by Hjellming & Webbink (1987; see also Hjellming 1989). This situation is encountered if a strong mass loss by wind steadily reducing the mass of the AGB star reversed the mass ratio prior to the onset of RLOF. Tout & Eggleton (1988) have shown that the mass ratio is easily reversed if the mass loss rate of the AGB star is tidally enhanced by the companion ('Companion-Reinforced Attrition Process', CRAP) so to exceed the Reimers rate by one or two orders of magnitude. By including this effect, Han et al. (1995) were able to stabilize the RLOF of many systems, which ended up as barium systems with periods in the range 250 – 2500 d.

Finally, the very concept of the Roche lobe may be irrelevant for systems involving a mass-losing star where the wind-driving force may substantially reduce the effective gravity of the mass-losing star (see the discussion in Theuns & Jorissen 1993). The existence of an extra-force driving the mass loss will clearly modify the shape of the equipotential surfaces, as shown by Schuerman (1972). The geometry of X-ray binaries involving mass-losing supergiants (Bolton 1975; Kondo et al. 1976), and possibly also of the yellow symbiotic-barium star BD$-21^\circ 3873$ (Smith et al. 1997), are indeed observed to deviate from the predictions made with the usual Jacobi integral describing the restricted three-body equipotential surfaces. In particular, if the effective gravity is reduced below some threshold depending upon the mass ratio, the critical Roche equipotential will degenerate into a surface including *both* the Lagrangian points L_1 and L_2 (if the mass-losing star is the more massive component) or L_1 and L_3 (in the opposite case). Matter will thus not necessarily be confined to the lobe surrounding the accreting component, but may escape from the system through L_2 or L_3, after forming a circumbinary disk. Furthermore, in the case of a strong wind, the particles have initially non-zero kinetic energy taken from the internal energy of the mass-losing star, that makes the equipotentials escapable barriers. Therefore, only a limited fraction of the mass lost by the AGB star is accreted by the companion, and such a reduced accretion rate will be less prone to trigger the expansion of the accreting star envelope, at the origin of the common envelope formation. The mass flows in these situations are complex, as shown by recent *Smooth Particle Hydrodynamics* simulations (Theuns & Jorissen 1993; Theuns et al. 1996).

12. Do S stars evolve from barium stars?

The orbital properties of S stars appear to be identical to those of barium stars, as apparent from Fig. 4 [$(e, \log P)$ diagram] and Figs. 8 and 10 (mass-function distribution). This similarity is a strong indication that binary S stars are simply the descendants of barium stars as they cool while ascending either the RGB or the E-AGB[6]. Because the evolution is slower on the RGB than on the E-AGB, it may actually be expected that binary S stars be dominated by stars on the upper RGB rather than on the E-AGB. In this case, *they ought to be low-mass stars* (because only low-mass stars develop a red giant branch), in agreement with the value 1.6 $M_\odot$ derived from their average Q (Table 9).

It is expected that at some point in their evolution on the RGB the S stars with the shortest periods ($P \lesssim 600$ d) will overflow their Roche lobe. In that respect, it should be noted that the hottest (i.e. least evolved) S star in our sample, HD 121447, has the shortest period among S stars. The detailed analysis of this system performed by Jorissen et al. (1995) concludes that the giant will overflow its Roche lobe before reaching the RGB-tip, with a dramatic fate for the binary system as described in Sect. 11 in relation with unstable case C mass transfer. The various processes that prevented the orbital decay of the binary system in a former stage of its evolution, when the AGB progenitor of the present WD filled its Roche lobe, are no longer applicable to this second RLOF event. First, the mass ratio can no longer be inverted easily, as the companion is already a low-mass WD, so that case C mass transfer is necessarily dynamically unstable. Second, the envelope of a RGB star is more tightly bound than that of an evolved AGB star (since it is less extended and its 'gravity-reducing' wind is much weaker), so that more energy has to be extracted from the orbit to expell the common envelope, resulting in a stronger orbital decay. A lack of short-period S systems is predicted from these considerations, as already suspected by Jorissen & Mayor (1992). This effect is not immediately apparent from the comparison between the cumulative period distributions of barium and S stars (Fig. 5). However, there are good reasons to suspect that the two shortest-period S systems, HD 121447 and HD 191589, are peculiar in some respect (HD 121447: see above; HD 191589 is a puzzling Tc-poor S star with an A-type companion, see Sect. 9.2). If these special cases are removed from the sample of S stars, S systems with $P \lesssim 600$ d appear to be lacking, in agreement with the critical periods expected for RLOF on the upper RGB (see Table 5 of Jorissen & Mayor 1992).

13. Related families: dwarf barium stars, post-AGB stars, symbiotic stars

Possible links between the PRG families considered in this paper and symbiotic stars, post-AGB stars and dwarf barium stars are briefly considered in this section.

13.1. Dwarf barium stars

Most barium stars may be expected to form as dwarf stars, since the stellar lifetime is longer on the main sequence than on the giant branch, and since the cross section for wind accretion is independent of the geometric radius of the star according to the Bondi-Hoyle formula (Eq. 5). Dwarf barium stars long

[6] Strictly speaking, the S and barium phases may even be intermingled in the sequence Ba (lower RGB) - S (upper RGB) – Ba (He clump) – S (E-AGB and TP-AGB)

remained elusive, until Luck & Bond (1982, 1991) and North et al. (1994) recognized that some of the CH subgiants previously identified by Bond (1974), as well as some of the F dwarfs previously classified by Bidelman (1985) as having a 'strong Sr $\lambda 4077$' line, had the proper abundance anomalies, gravities and galactic frequencies to be identified with the long- sought Ba dwarfs. A large fraction of binaries (about 90%) has been found among the stars with strong anomalies, as expected (McClure 1985; North et al. 1997). The suspected WD companions to these dwarf barium stars appear to be too cool to be detectable with the IUE satellite (Bond 1984; North & Lanz 1991).

On the contrary, it is the presence of a hot WD companion to the K dwarf 2RE J0357+283 that led Jeffries & Stevens (1996) to suspect it might be a dwarf barium star. A subsequent spectroscopic analysis (Jeffries & Smalley 1996) confirmed this early suspicion. This star is the first example of the new class of WIRRing ('Wind-Induced Rapidly Rotating') stars, that have been spun up by wind accretion, as predicted by SPH simulations (Theuns et al. 1996). The giant barium star HD 165141, which has a hot WD companion as well (Fekel et al. 1993), is another member of that class (Jorissen et al. 1996).

13.2. Post-AGB stars

The post-AGB stars with large Fe deficiencies studied by Van Winckel et al. (1995) are all binaries, and their $(e, \log P)$ diagram is very similar to that of barium stars (Van Winckel et al. 1997). These post-AGB stars could be related to barium stars, were it not for the absence of clear evidence for s-process enrichment of these stars (Van Winckel 1995).

13.3. Yellow symbiotic stars

Symbiotic systems consist of a late-type giant and a hot companion, a WD in most cases, exhibiting nebular lines in their spectra (e.g. Kenyon 1986). Yellow symbiotics involve a G or K giant and are often halo objects (Schmid & Nussbaumer 1993). Many exhibit the barium syndrome (UKS-Ce1 and S32: Schmid 1994; AG Dra: Smith et al. 1996; BD$-21^\circ 3873$: Smith et al. 1997), which must have formed in much the same way as in barium and S systems. These yellow symbiotics are probably evolving on the upper RGB or on the E-AGB, thus being the Pop.II counterparts of the extrinsic S stars, whereas the hotter CH stars would be the analogs of the barium stars. A more detailed comparison can be found in Jorissen (1997).

14. Conclusions

Radial-velocity monitoring of a complete sample of barium stars with strong anomalies reveals that 35 out of 37 stars show clear evidence of binary motion. For mild barium stars, that frequency amounts to 34/40 (or 37/40 if one includes the suspected binaries). A Monte-Carlo simulation shows that these frequencies are compatible with the hypothesis that *all* the observed stars are binary systems, some of them remaining undetected because of unfavourable orbital orientation or time sampling. We conclude therefore that there is no need to invoke a barium-star formation mechanism other than one (like mass transfer) directly related to the binary nature of these stars. In other words, *binarity appears to be a necessary condition to form a barium star*. It seems, however, that it is not a sufficient condition, since binary systems with barium-like orbital elements but no heavy-element overabundances seem to exist (e.g. DR Dra). It has been argued that a metallicity lower than solar may be the other parameter required to form a barium star. The increasing levels of heavy-element overabundances observed in the sequence mild Ba – strong Ba – CH stars support that hypothesis, since this sequence is also one of increasing age (and thus, to first order, of decreasing metallicity), as revealed by their kinematical properties.

The $(e, \log P)$ diagram of PRG stars clearly shows the signature of mass transfer, since the maximum eccentricity observed at a given orbital period is much smaller than in a comparison sample of normal giants in clusters. Mass transfer rather than some non-standard internal mixing induced by binarity must thus be held responsible for the chemical peculiarities exhibited by PRG stars. A distinctive feature of the $(e, \log P)$ diagram of barium stars is the presence of two distinct modes: a short-period mode ($P \lesssim 1500$ d) comprising nearly-circular orbits ($e < 0.08$), populated by strong barium stars only, and a long-period mode made exclusively of non-circular orbits. At this point, it is not clear whether the nearly circular orbits of the short-period mode bear the signature of RLOF, or whether they arise from tidal circularization on the RGB long after the mass-transfer process. Detailed models of binary evolution are required to answer that question.

The comparison of the mass-function distributions of mild and strong barium stars confirms that the difference between them is mainly one of galactic population rather than of orbital separation, since mild barium stars host more massive giants than strong barium stars. The loose correlation that is observed between the orbital period and the level of heavy-element overabundances is another indication that a parameter not directly related to the orbital dynamics has a strong impact on the pollution level of the barium star. All these facts fit together nicely if the s-process operation is more efficient in a low-metallicity population. Provided that the reaction $^{13}\mathrm{C}(\alpha, \mathrm{n})^{16}\mathrm{O}$ is the neutron source responsible for the operation of the s-process, such a correlation between metallicity and s-process efficiency is indeed predicted on very general theoretical grounds. In this framework, the giant star in Pop.II CH systems has accreted material much enriched in heavy elements by its former AGB companion. Therefore, stars of old, low-metallicity populations like CH stars (and to a lesser extent, strong barium stars) exhibit, *for a given orbital period*, much larger heavy-element overabundances than stars belonging to a younger population.

A radial-velocity monitoring of S stars confirms that Tc-poor S stars are all binaries and are the cool descendants of the barium stars on the RGB or E-AGB, since they have similar orbital periods and mass functions. There is a suggestion, however, that the short-period tail of S stars may be truncated at about 600 d due to RLOF occurring on the upper RGB. Similarly, for Pop.II stars, yellow barium-symbiotic systems like AG Dra

and BD$-21°3873$ are the cool descendants of the hotter CH stars. Two Tc-poor S stars, HDE 332077 and HD 191589, have unusually large mass functions, and an A-type companion has been detected in both cases with IUE, as well as in 57 Peg (Van Eck et al. 1998). The evolutionary status of these stars is currently unclear.

Acknowledgements. This paper was written in part when A.J. was *Visiting Research Fellow* at the Department of Astrophysical Sciences at Princeton University. Financial support from the *Fonds National de la Recherche Scientifique* (Belgium, Switzerland) is gratefully acknowledged. S.V.E. is Boursier F.R.I.A. (Belgium) and was partly supported by a grant from the Société Suisse d'Astronomie during a stay at the Observatoire de Genève. The operation of the CORAVEL spectrovelocimeter has been possible thanks to financial support from the *Fonds National Suisse de la Recherche Scientifique*.

Appendix A: setting up a photometric index probing the chemical peculiarities in barium stars

To be able to compare in a homogeneous way the level of chemical peculiarities in different barium stars is clearly of paramount importance when trying to identify the mass transfer scenario that operated in these stars. A key constraint may indeed be obtained by assessing whether or not there is a correlation between the level of chemical peculiarities and some dynamical parameter like the orbital period. As detailed abundance analyses are only available for a small subset of barium stars, the aim of this Appendix is to design a photometric index available for (nearly) all barium stars and probing their chemical peculiarities.

Lü et al. (1983) and Lü (1991) pointed out that barium stars segregate according to their Ba index (as defined in the scale of Warner 1965 from visual inspection of the strength of the Ba$\lambda 4554$ line) in the $[C(38-41), C(42-45)]$ color-color diagram constructed from DDO photometric indices (see McClure & van den Bergh 1968). This segregation is caused by the so-called Bond-Neff depression, a broad absorption feature present in the spectrum of barium stars and extending from about 350 to 450 nm (Bond & Neff 1969; Lü & Sawyer 1979). A veil of many heavy-element lines has been proposed as the origin of this broad feature (McWilliam & Smith 1984; Wing 1985, and references therein), though that issue is still controversial as CN bands are also important contributors in this spectral region (Tripicco & Bell 1991).

According to these findings, it may be expected that a photometric index of the form $\Delta(38-41) = C(38-41) - mC(42-45) + n$ be related to the level of chemical peculiarities in barium stars (see Fig. 4 of Lü 1991). The m and n parameters in the above relation may actually be chosen so as to yield the maximum correlation between $\Delta(38-41)$ and some given abundance indicator. McWilliam (1988, 1990) showed that the abundance ratio YII/TiII, derived from the YII $\lambda 6795.4$ and TiII $\lambda 6607.0$ lines, is a powerful indicator for detecting heavy-element abundance peculiarities in red giants, since (i) that abundance ratio is relatively insensitive to the atmospheric parameters, and (ii) the distribution of YII/TiII ratios in a sample of about 600 G – K giants is very narrow, with a FWHM of only 0.3 dex centered at log(YII/TiII) $= -2.75$ (adopted as normalization value for [YII/TiII] in the following).

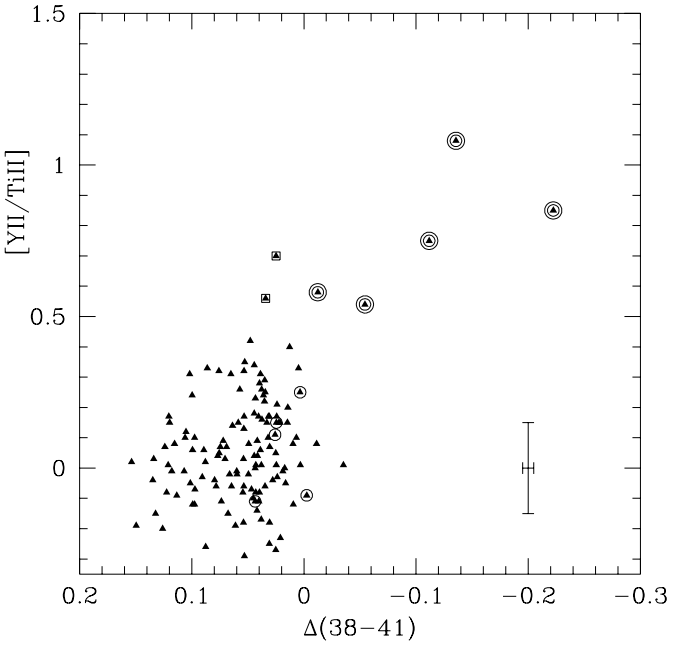

Fig. A.1. The $\Delta(38-41)$ color index vs. [YII/TiII] for 131 G – K giants with DDO colors from McClure & Forrester (1981) and abundances from McWilliam (1990). Typical error bars have been indicated. Double-circled triangles identify the barium stars HD 116713, HD 139195, HD 204075, HD 202109 and HD 212320, whereas squares correspond to heavy element-rich stars according to McWilliam (1990), not previously reported as barium stars (see text). Strong CN stars from the list of Keenan, Yorka & Wilson (1987) have been represented by single-circled triangles

The $\Delta(38-41)$ index has therefore been calibrated in terms of [YII/TiII] abundances, using 131 G and K giants for which both DDO colors (McClure & Forrester 1981) and abundances (McWilliam 1990) are available.

The value $m = 0.90$ is obtained by requiring maximum linear correlation between [Y/Ti] and $\Delta(38-41)$ for that sample, and $n = 1.33$ ensures that barium stars have $\Delta(38-41) < 0$, whereas nearly all normal giants have $\Delta(38-41) \geq 0$ (Fig. A.1).

Although the expected trend is clearly present (taking into account the ~ 0.2 dex uncertainty on [Y/Ti]), there are a few stars in 'forbidden' regions [namely (i) non-barium stars [Y/Ti]< 0.5 with $\Delta(38-41) < 0$, or (ii) possible barium stars [Y/Ti]> 0.5 with $\Delta(38-41) \geq 0$], degrading the ability of the $\Delta(38-41)$ index to identify barium stars. The two stars (HR 7754 and HR 8590) in region (ii) were not previously identified as barium stars. HR 7754 is in fact present in the list of MK standards provided by Keenan & McNeil (1989), and there is no mention whatsoever of the barium nature of that star, classified as G9III. Apart from the fact that HR 7754 is member of

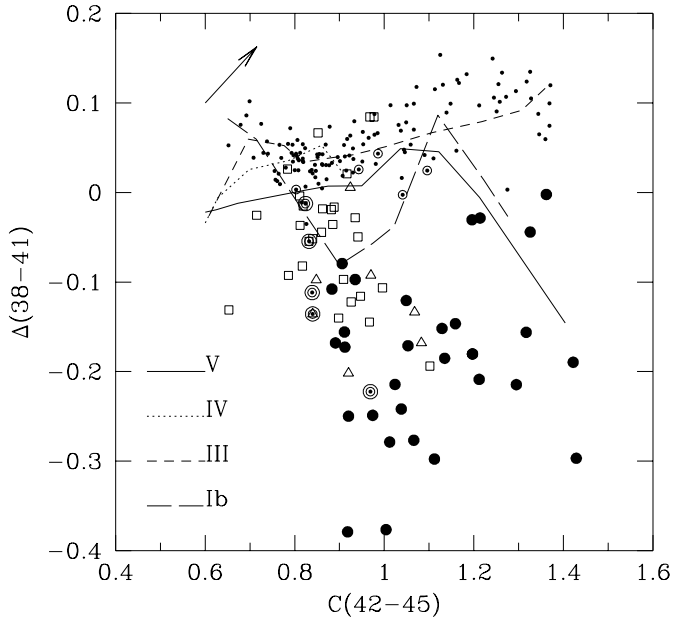

Fig. A.2. The $\Delta(38-41)$ color index vs. $C(42-45)$ for barium stars (open squares: Ba0 – Ba1, open triangles: Ba2 – Ba3, filled circles: Ba4 – Ba5). The loci of main sequence stars (class V), subgiant stars (class IV), giant stars (class III) and supergiant stars (class Ib), as provided by McClure & Forrester (1981), are indicated by the various lines. Small dots correspond to 131 G – K giants common to the samples of McClure & Forrester (1981) and McWilliam (1990), as plotted in Fig. A.1. Double-circled and single-circled symbols identify the same stars as in Fig A.1. The arrow corresponds to a reddening by $E_{\rm B-V} = 0.5$

a complex multiple visual system, there is currently no clue as to the origin of this discrepancy.

Stars in region (i) ([Y/Ti]< 0.5, $\Delta(38-41) < 0$) may actually be bright giants or CN-strong stars, spilling somewhat over into the region of barium stars. It is indeed clear from the $[C(42-45), \Delta(38-41)]$ diagram (Fig. A.2), where the fiducial loci of dwarfs, giants and Ib supergiants from McClure & Forrester (1981) have been indicated, that Ib supergiants with $\Delta(38-41) < -0.1$ may be found among barium stars. As CN bands are strong contributors to the the $C(38-41)$ index (Tripicco & Bell 1991), CN-strong stars tend to have $\Delta(38-41)$ indices smaller than average as well, and some (like HR 3905) may also contaminate region (i) (Fig. A.2).

No reddening correction has been applied to the stars plotted in Fig. A.2. According to the reddening correction factors provided by McClure (1979), reddening is expected to have a very limited impact on the $\Delta(38-41)$ index, as the de-reddened index writes $\Delta_0(38-41) = \Delta(38-41) - 0.13 E_{\rm B-V}$.

Despite ambiguities in identifying barium stars when $\Delta(38-41)$ is close to 0, smaller values of that index correlate fairly well with heavy-element overabundances, as indicated by the barium stars present in Fig. A.1. In fact, a similar correlation was already obtained for the closely-related Δc_1 index defined by Jorissen et al. (1992b) from Strömgren photometry.

With the adopted normalization, mild barium stars typically have $-0.1 \lesssim \Delta(38-41) \lesssim 0$ while strong barium stars (with Ba4 and Ba5 indexes) have $\Delta(38-41) \lesssim -0.1$.

References

Ake T.B., 1979, ApJ 234, 538
Ake T.B., 1997. In: Wing R. (ed.) The Carbon Star Phenomenon (IAU Symp. 177) Kluwer, Dordrecht, in press
Ake T.B., Johnson H.R., 1988, ApJ 327, 214
Ake T.B., Johnson H.R., Ameen M.M., 1991, ApJ 383, 842
Ake T.B., Johnson H.R., 1992. In: Giampapa M.S., Bookbinder J.A. (eds.) Seventh workshop on cool stars, stellar systems and the sun. Astron. Soc. Pacific Conf. Ser. 26, p.579
Ake T.B., Jorissen A., Johnson H.R., Mayor M., Bopp B., 1992, Bull. Am. Astron. Soc. 24, 1280
Baranne A., Mayor M., Poncet J.L., 1979, Vistas in Astron. 23, 279
Barbier M., Mayor M., Menessier M.O., Petit H., 1988, A&AS 72, 463
Berdyugina S.V., 1994, Pi'sma Astron. J. 20, 910
Bergeat J., Knapik A., 1997, A&A 321, L9
Bidelman W.P., 1985, AJ 90, 341
Bidelman W.P., Keenan P.C., 1951, ApJ 114, 473
Boffin H.M.J., Jorissen A., 1988, A&A 205, 155
Boffin H.M.J., Cerf N., Paulus G., 1993, A&A 271, 125
Böhm-Vitense E., Johnson H.R., 1985, ApJ 293, 288
Bolton C.T., 1975, ApJ 200, 269
Bond H.E., 1974, ApJ 194, 95
Bond H.E., 1984. In: Mead J.-M., Chapman R.D., Kondo Y. (eds.) Future of Ultraviolet Astronomy based on six years of IUE Research. NASA CP 2349, NASA, Greenbelt, p. 289
Bond H.E., Neff J.S., 1969, ApJ 158, 1235
Bondi H., Hoyle F., 1944, MNRAS 104, 273
Brown J.A., Smith V.V., Lambert D.L., Dutchover E., Hinkle K.H., Johnson H.R., 1990, AJ 99, 1930
Burbidge E.M., Burbidge G.R., Fowler W.A., Hoyle F., 1957, Rev. Mod. Phys. 29, 4
Busso M., Lambert D.L., Beglio L., Gallino R., Raiteri C.M., Smith V.V., 1995, ApJ 446, 775
Carquillat J.M., Jorissen A., Udry S., Ginestet N., 1998, A&A, in press
Catchpole R.M., Robertson B.S.C., Warren P.R., 1977, MNRAS 181, 391
Cerf N., Boffin H.M.J., 1994, Inverse Problems 10, 533
Clayton D.D., 1988, MNRAS 234, 1
Culver R.B., Ianna P.A., 1975, ApJ 195, L37
de Kool M., 1992, A&A 261, 188
Duquennoy A., Mayor M., 1991, A&A 248, 485
Duquennoy A., Mayor M. (eds.), 1992, Binaries as tracers of stellar formation. Cambridge Univ. Press, Cambridge
Duquennoy A., Mayor M., Mermilliod J.-Cl., 1992. In: Duquennoy A., Mayor M. (eds.) Binaries as tracers of stellar formation. Cambridge Univ. Press, Cambridge, p. 52
ESA, 1997. The Hipparcos and Tycho Catalogues, ESA-SP 1200
Feast M.W., 1953, MNRAS 113, 510
Fekel F.C., Henry G.W., Busby M.R., Eitter J.J., 1993, AJ 106, 2370
Gray R.F., 1988, Lectures on spectral-line analysis: F, G and K stars, The Publisher, Arva (Ontario)
Griffin R.F., 1984, The Observatory 104, 224
Griffin R.F., 1991, The Observatory 111, 29
Griffin R.F., 1996, The Observatory 116, 398
Griffin R., Griffin R., 1980, MNRAS 193, 957
Griffin R.F., Keenan P.C., 1992, The Observatory 112, 168

Griffin R.F., Jorissen A., Mayor M., 1996, The Observatory 116, 298
Groenewegen M.A.T., 1993, A&A 271, 180
Hackos W.Jr., Peery B.F.Jr., 1968, AJ 73, 504
Han Z., Eggleton P.P., Podsiadlowski P., Tout C.A., 1995, MNRAS 277, 1443
Herbig G.H., 1965, Kleine Veroff. Remeis-Sternwarte 4, Nr 40, 164
Hjellming M.S., 1989, Ph.D. thesis, Univ. Illinois, Urbana-Champaign
Hjellming M.S., Webbink R.F., 1987, ApJ 318, 794
Iben I.Jr., Renzini A., 1983, ARA&A 21, 271
Iben I.Jr., Livio M., 1993, PASP 105, 1373
Iben I.Jr., Tutukov A.V., 1993, ApJ 418, 343
Jeffries R.D., Stevens I.R., 1996, MNRAS 279, 180
Jeffries R.D., Smalley B., 1996, A&A 315, L19
Johnson H.R., 1992. In: Kondo Y., Sistero R.F., Polidan R.S. (eds.) Proc. IAU Symp. 151, Evolutionary Processes in Interacting Binary Stars. Kluwer, Dordrecht, p. 157
Johnson H.R., Ake T.B., Ameen M.M., 1993, ApJ 402, 667
Jorissen A., 1997. In: J. Mikolajewska (ed.) Physical Processes in Symbiotic Binaries and Related Systems, Publ. Copernicus Foundation for Polish Astron., Warsaw, p. 135
Jorissen A., Mayor M., 1988, A&A 198, 187
Jorissen A., Mayor M., 1992, A&A 260, 115
Jorissen A., Boffin H.M.J., 1992. In: Duquennoy A., Mayor M. (eds.) Binaries as tracers of stellar formation. Cambridge Univ. Press, Cambridge, p. 110
Jorissen A., Smith V.V., Lambert D.L., 1992a, A&A 261, 164
Jorissen A., Manfroid J., Sterken C., 1992b, A&A 253, 407
Jorissen A., Frayer D.T., Johnson H.R., Mayor M., Smith V.V., 1993, A&A 271, 463
Jorissen A., Hennen O., Mayor M., Bruch A., Sterken Ch., 1995, A&A 301, 707
Jorissen A., Schmitt J.H.M.M., Carquillat J.M., Ginestet N., Bickert K.F., 1996, A&A 306, 467
Keenan P.C., 1942, ApJ 96, 101
Keenan P.C., 1950, AJ 55, 172
Keenan P.C., Wilson O.C., 1977, ApJ 214, 399
Keenan P.C., McNeil R.C., 1989, ApJS 71, 245
Keenan P.C., Yorka S.B., Wilson O.C., 1987, PASP 99, 629
Kenyon S.J., 1986. The Symbiotic Stars, Cambridge Univ. Press
Kholopov P.N., Samus' N.N., Frolov M.S., et al., 1985. General Catalogue of Variable Stars (4th edition). Nauka, Moscow
Kipper T., Jo rgensen U.G., Klochkova V.G., Panchuk V.E., 1996, A&A 306, 489
Kondo Y., McCluskey G.E. Jr., Gulden S.L., 1976. In: X-ray Binaries, Boldt E., Kondo Y. (eds.) NASA-SP 389, Washington D.C., p. 499
Kovács N., 1985, A&A 150, 232
Kukarkin B. V, Kholopov P. N., Artiukhina N. M., et al., 1982. New General Catalogue of Suspected Variable Stars. Nauka, Moscow
Lambert D.L., 1985. In: Jaschek M., Keenan P.C. (eds.) Cool Stars with Excesses of Heavy Elements. Reidel, Dordrecht, p.191
Lambert D.L., Smith V.V., Heath J., 1993, PASP 105, 568
Little S.J., Little-Marenin I.R., Hagen-Bauer W., 1987, AJ 94, 981
Lü P.K., 1991, AJ 101, 2229
Lü P.K., Dawson D.W., Upgren A.R., Weis E.W., 1983, ApJS 52, 169
Lü P.K., Sawyer D., 1979, ApJ 231, 144
Lubow S.H., Artymowicz P., 1992. In: Duquennoy A., Mayor M. (eds.) Binaries as tracers of stellar formation. Cambridge Univ. Press, Cambridge, p. 145
Luck R.E., Bond H.E., 1982, ApJ 259, 792
Luck R.E., Bond H.E., 1991, ApJS 77, 515
Lucy L.B., Sweeney M.A., 1971, AJ 76, 544
Mayor M., Imbert M., Andersen J., Ardeberg A., Benz W., Lindgren H., Martin N., Maurice E., Nordström B., Prévot L., 1984, A&A 134, 118
Mazeh T., 1990, AJ 99, 675
Mazeh T., Shaham J., 1979, A&A 77, 145
McClure R.D., 1979. In: Davis Philip A.G. (ed.) Problems of calibration of multicolor photometric systems. Dudley Observ. Rep., Schenectady (New York), USA, p.83
McClure R.D., 1983, ApJ 268, 264
McClure R.D., 1984a, ApJ 280, L31
McClure R.D., 1984b, PASP 96, 117
McClure R.D., 1985. In: M. Jaschek & P.C. Keenan (eds.) Cool Stars with Excesses of Heavy Elements. Reidel, Dordrecht, p. 159
McClure R.D., Fletcher J.M., Nemec J.M., 1980, ApJ 238, L35
McClure R.D., Forrester W.T., 1981, Publ. Dominion Astrophys. Obs. 15, 439
McClure R.D., Forrester W.T., Gibson J., 1974, ApJ 189, 409
McClure R.D., van den Bergh S., 1968, AJ 73, 313
McClure R.D., Woodsworth A.W., 1990, ApJ 352, 709
McWilliam A., 1988, Ph.D. thesis, University of Texas at Austin
McWilliam A., 1990, ApJS 74, 1075
McWilliam A., Smith V.V., 1984, Bull. Am. Astron. Soc. 16, 973
Mennessier M.O., Luri X., Figueras F., Gómez A.E., Grenier S., Torra J., North P., 1997, A&A 326, 722
Mermilliod J.-C., 1996. In: G. Milone & J.-C. Mermilliod (eds.) The Origins, Evolution, and Destinies of Binary Stars in Clusters, ASP Conf. Ser. (in press)
Mermilliod J.-C., Mayor M., 1996. In: Pallavicini R., Dupree K. (eds.) Ninth Cambridge Workshop on Cool Stars, Stellar Systems and the Sun. ASP Conf. Ser. 109, p. 373
Merrill P.W., 1956, PASP 68, 162
Meyer F., Meyer-Hofmeister E., 1979, A&A 78, 167
North P., Lanz T., 1991, A&A 251, 489
North P., Berthet S., Lanz T., 1994, A&A 281, 775
North P., Jorissen A., Mayor M., 1997. In: R. Wing (ed.) The Carbon Star Phenomenon (IAU Symp. 177) Kluwer, Dordrecht, in press
Pastetter L., Ritter H., 1989, A&A 214, 186
Perraud H., 1959, J. Observateurs 42, 142
Press W. H., Teukolsky S. A., Vetterling W. T., Flannery B. P., Numerical Recipes in Fortran, Second Edition, 1992, Cambridge University Press
Reid I.N., 1996, AJ 111, 2000
Ritter H., 1996. In: Wijers R.A.M.J., Davies M.B., Tout C.A. (eds.) Evolutionary Processes in Binary Stars. Kluwer, Dordrecht, p.223
Sackmann I.-J., Boothroyd A.I., 1991. In: G. Michaud & A. Tutukov (eds.) Evolution of Stars: The Photospheric Abundance Connection (IAU Symp. 145) Kluwer, Dordrecht, p. 275
Scalo J.M., 1976, ApJ 206, 474
Schindler M., Stencel R.E., Linsky J.L., Basri G.S., Helfand D.J., 1982, ApJ 263, 269
Schmid H.M., 1994, A&A 284, 156
Schmid H.M., Nussbaumer H., 1993, A&A 268, 159
Schuerman D.W., 1972, Ap&SS 19, 351
Smith V.V., 1984, A&A 132, 326
Smith V.V., Lambert D.L., 1987, MNRAS 226, 563
Smith V.V., Lambert D.L., 1988, ApJ 333, 219
Smith V.V., Cunha K., Jorissen A., Boffin H.M.J., 1996, A&A 315, 179
Smith V.V., Cunha K., Jorissen A., Boffin H.M.J., 1997, A&A 324, 97
Sneden C., Lambert D.L., Pilachowski C.A., 1981, ApJ 247, 1052
Stephenson C.B., 1973. A General Catalogue of Cool Carbon Stars, Publ. Warner & Swasey Observ. 1, 4

Stephenson C.B., 1984. The General Catalogue of Galactic S Stars, Publ. Warner & Swasey Observ. 3, 1
Theuns T., Jorissen A., 1993, MNRAS 265, 946
Theuns T., Boffin H.M.J., Jorissen A., 1996, MNRAS 280, 1264
Tomkin J., Lambert D.L., 1986, ApJ 311, 819
Tout C.A., Eggleton P.P., 1988, MNRAS 231, 823
Tripicco M.J., Bell R.A., 1991, AJ 102, 744
Udry S., Mayor M., Van Eck S., Jorissen A., 1998a, A&AS, in press
Udry S., Mayor M., Van Eck S., Jorissen A., Prévot L., Lindgren H., 1998b, A&AS, in press
Utsumi K., 1985. In: Jaschek M., Keenan P.C. (eds.) Cool Stars with Excesses of Heavy Elements. Reidel, Dordrecht, p.243
van Belle G.T., Dyck H.M., Benson J.A., Lacasse M.G., 1996, AJ 112, 2147
Van Eck S., Jorissen A., Udry S., Mayor M., Pernier B., 1998, A&A 329, 971
Van Winckel H., 1995. PhD. thesis, Kathol. Univ. Leuven
Van Winckel H., Waelkens C., Waters L.B.F.M, 1995, A&A 293, L25
Van Winckel H., Waelkens C., Jorissen A., Van Eck S., North P., Waters R., 1997. In: Wing R. (ed.) The Carbon Star Phenomenon (IAU Symp. 177) Kluwer, Dordrecht, in press
Vanture A.D., 1992, AJ 104, 1997
Vissotsky A.N., Balz A.G.A., 1958, Publ. McCormick Obs. 13, pt.2
Warner B., 1965, MNRAS 129, 263
Webbink R.F., 1986. In: Leung K.C., Zhai D.S. (eds.) Critical Observations vs Physical Models for Close Binary Systems. Gordon and Breach, New York, p. 403
Wing R. F., 1985. In: Jaschek M., Keenan P.C. (eds.) Cool Stars with Excesses of Heavy Elements. Reidel, Dordrecht, p. 61
Začs L., 1994, A&A 283, 937
Začs L., Musaev F.A., Bikmaev I.F., Alksnis O., 1997, A&AS 122, 31